Inorganic Chemistry B

Chapter 21

d-Block metal chemistry: coordination complexes

21.1 Introduction

In this chapter, we discuss complexes of the *d*-block metals and we consider bonding theories that rationalize experimental facts such as ***electronic spectra*** and ***magnetic properties***.

Most of our discussion centers on **first row** *d*-block metals, for which theories of bonding are most successful.

Fundamental to discussions about d-block chemistry are the **3*d***, **4*d*** or **5*d*** orbitals for the ***first***, ***second*** or ***third*** row *d*-block metals, respectively.

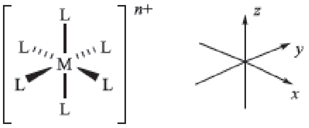

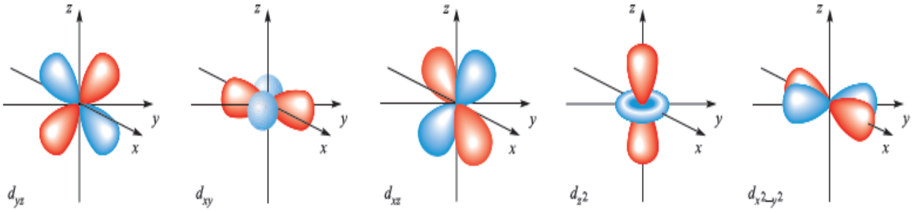

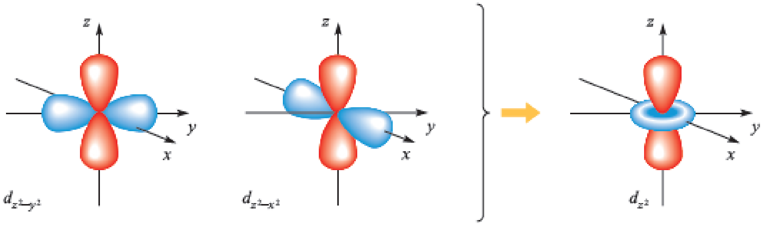

High- and low-spin states

Magnetic data allow us to determine the number of *unpaired electrons*.

In an isolated first row d-block metal ion, the 3d orbitals are degenerate and the electrons occupy them according to Hund's rules: e.g. diagram **21.1** shows the arrangement of six electrons.

(21.1)

However, magnetic data for a range of octahedral ***d*^{6}** complexes show that they fall into two categories:

- Paramagnetic **high-spin** complexes and correspond to those in which, despite the d orbitals being split, there are still four **unpaired electrons**
- Diamagnetic **low-spin** and correspond to those in which electrons are **doubly occupying** three orbitals, leaving two unoccupied.

High- and **low-spin** complexes exist for octahedral d^4, d^5, d^6 and d^7 metal complexes.

For d^4, d^5 and d^7 configurations, both **high**- and **low-spin** complexes of a given configuration are **paramagnetic**, but with different numbers of unpaired electrons.

21.2 Bonding in d-block metal complexes: valence bond theory

Hybridization schemes

Applications of these hybridization schemes to describe the bonding in *d*-block metal complexes

An empty hybrid orbital on the metal center can accept a pair of electrons from a ligand to form **σ -bond**.

Table ation schemes for the σ-bonding frameworks of different geometrical configurations of ligand donor atoms.

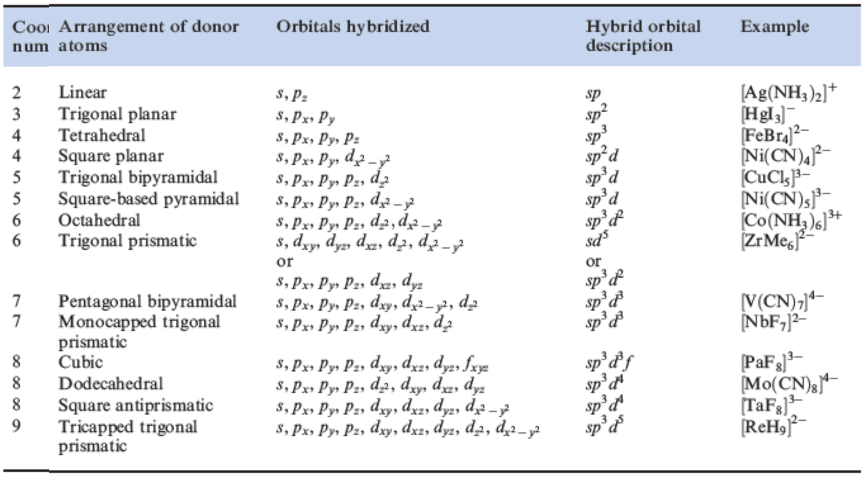

Coo num	Arrangement of donor atoms	Orbitals hybridized	Hybrid orbital description	Example
2	Linear	s, p_z	sp	$[Ag(NH_3)_2]^+$
3	Trigonal planar	s, p_x, p_y	sp^2	$[HgI_3]^-$
4	Tetrahedral	s, p_x, p_y, p_z	sp^3	$[FeBr_4]^{2-}$
4	Square planar	$s, p_x, p_y, d_{x^2-y^2}$	sp^2d	$[Ni(CN)_4]^{2-}$
5	Trigonal bipyramidal	$s, p_x, p_y, p_z, d_{z^2}$	sp^3d	$[CuCl_5]^{3-}$
5	Square-based pyramidal	$s, p_x, p_y, p_z, d_{x^2-y^2}$	sp^3d	$[Ni(CN)_5]^{3-}$
6	Octahedral	$s, p_x, p_y, p_z, d_{z^2}, d_{x^2-y^2}$	sp^3d^2	$[Co(NH_3)_6]^{3+}$
6	Trigonal prismatic	$s, d_{xy}, d_{yz}, d_{xz}, d_{z^2}, d_{x^2-y^2}$ or $s, p_x, p_y, p_z, d_{xz}, d_{yz}$	sd^5 or sp^3d^2	$[ZrMe_6]^{2-}$
7	Pentagonal bipyramidal	$s, p_x, p_y, p_z, d_{xy}, d_{x^2-y^2}, d_{z^2}$	sp^3d^3	$[V(CN)_7]^{4-}$
7	Monocapped trigonal prismatic	$s, p_x, p_y, p_z, d_{xy}, d_{xz}, d_{z^2}$	sp^3d^3	$[NbF_7]^{2-}$
8	Cubic	$s, p_x, p_y, p_z, d_{xy}, d_{xz}, d_{yz}, f_{xyz}$	sp^3d^3f	$[PaF_8]^{3-}$
8	Dodecahedral	$s, p_x, p_y, p_z, d_{z^2}, d_{xy}, d_{xz}, d_{yz}$	sp^3d^4	$[Mo(CN)_8]^{4-}$
8	Square antiprismatic	$s, p_x, p_y, p_z, d_{xy}, d_{xz}, d_{yz}, d_{x^2-y^2}$	sp^3d^4	$[TaF_8]^{3-}$
9	Tricapped trigonal prismatic	$s, p_x, p_y, p_z, d_{xy}, d_{xz}, d_{yz}, d_{z^2}, d_{x^2-y^2}$	sp^3d^5	$[ReH_9]^{2-}$

The limitations of VB theory

considering octahedral complexes of Cr(III) (d^3) and Fe(III) (d^5) and octahedral, tetrahedral and square planar complexes of Ni(II) (d^8).

The atomic orbitals required for hybridization in an octahedral complex of a first row ***d*-block** metal are the $3d_{z^2}$, $3d_{x^2-y^2}$, $4s$, $4p_x$, $4p_y$ and $4p_z$ these orbitals must be ***unoccupied*** so as to be available to ***accept*** six pairs of electrons from the ligands.

The Cr^{3+} (d^3) ion has three unpaired electrons and these are accommodated in the $3d_{xy}$, $3d_{xz}$ and $3d_{yz}$ orbitals:

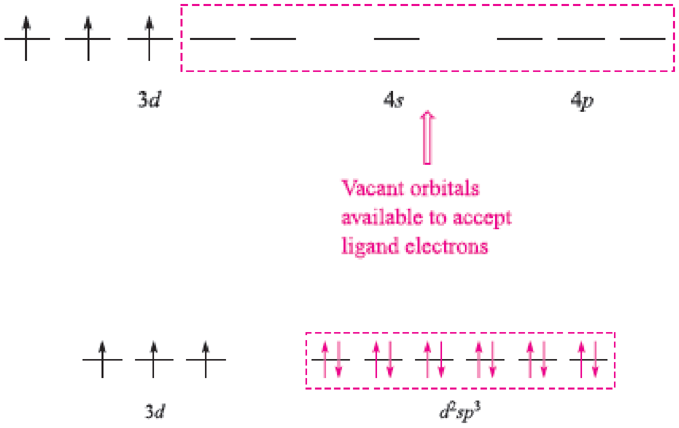

For octahedral Fe(III) complexes (d^5), we must account for the existence of both high- and low-spin complexes.
The electronic configuration of the free Fe^{3+} ion is:

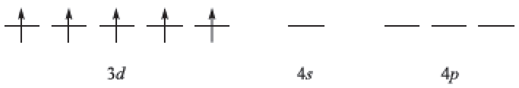

For a **low-spin** octahedral complex such as $[Fe(CN)_6]^{3-}$

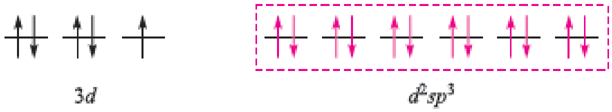

For a **high-spin** octahedral complex such as $[FeF_6]^{3-}$, the five 3d electrons occupy the five 3d atomic orbitals (as in the free ion shown above) and the two d orbitals required for the sp^3d^2 hybridization scheme must come from the 4d set.
With the ligand electrons included

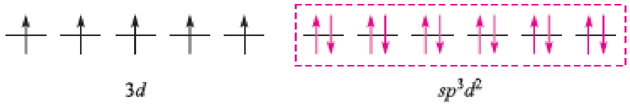

This scheme, however, is unrealistic because the 4d orbitals are at a significantly higher energy than the 3d atomic orbitals.

Nickel(II) (d^8) forms paramagnetic tetrahedral and octahedral complexes, and diamagnetic square planar complexes.

Bonding in a tetrahedral complex

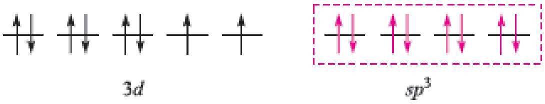

Bonding in an octahedral complex

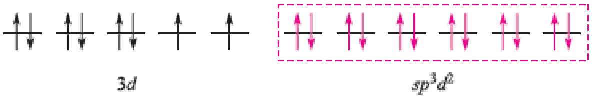

For diamagnetic *square planar* complexes, valence bond theory gives the following picture:

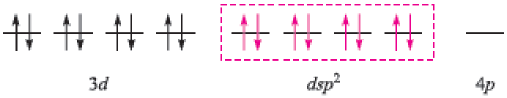

Valence bond theory may rationalize *stereochemical* and *magnetic properties*, but only at a simplistic level.

VBT, It can say nothing about

- electronic spectroscopic properties
- kinetic inertness (see Section 26.2) that is a characteristic of the low-spin d^6 configuration.
- why certain ligands are associated with the formation of high- (or low-)spin complexes.

21.3 Crystal field theory *an electrostatic model*

A second approach to the bonding in complexes of the d-block metals is **crystal field theory**.

- This is an electrostatic model and simply uses the ligand electrons to create an **electric field** around the **metal center**.
- Ligands are considered as point charges and there are no metal–ligand covalent interactions.

The octahedral crystal field

- Consider a first row metal cation surrounded by six ligands placed on the Cartesian axes at the vertices of an octahedron
- Each ligand is treated as a negative point charge and there is an electrostatic attraction between the metal ion and ligands.
- There is also a repulsive interaction between electrons in the ***d*** orbitals and the ligand point charges.

> If the electrostatic field (***the crystal field***) were spherical, then the energies of the five d orbitals would be raised (*destabilized*) by the same amount.

The octahedral crystal field

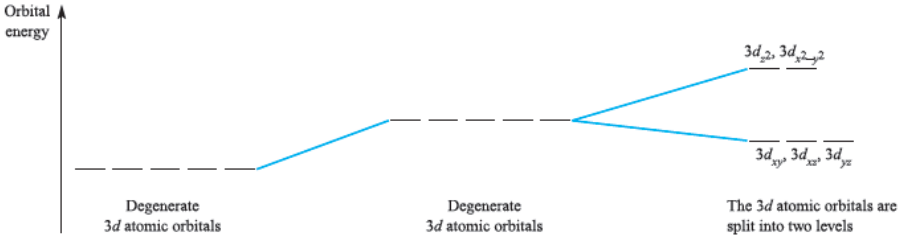

Metal ion M^{n+} and six ligands L at an infinite distance away

If the electrostatic field created by the point charge ligands is *spherical*, the energies of the electrons in the 3*d* orbitals are raised uniformly

octahedral crystal field

- The d_{z^2} and $d_{x^2-y^2}$ atomic orbitals point directly at the ligands
- The d_{xy}, d_{yz} and d_{xz} atomic orbitals point between them
- The d_{z^2} and $d_{x^2-y^2}$ atomic orbitals are *destabilized* to a greater extent than the d_{xy}, d_{yz} and d_{xz} atomic orbitals

Crystal field theory is an ***electrostatic model*** which predicts that the ***d*** orbitals in a metal complex are *not degenerate*. The *pattern of splitting* of the ***d*** orbitals depends on the crystal field, this being determined by the **arrangement** and **type** of **ligands**.

From the O_h character table

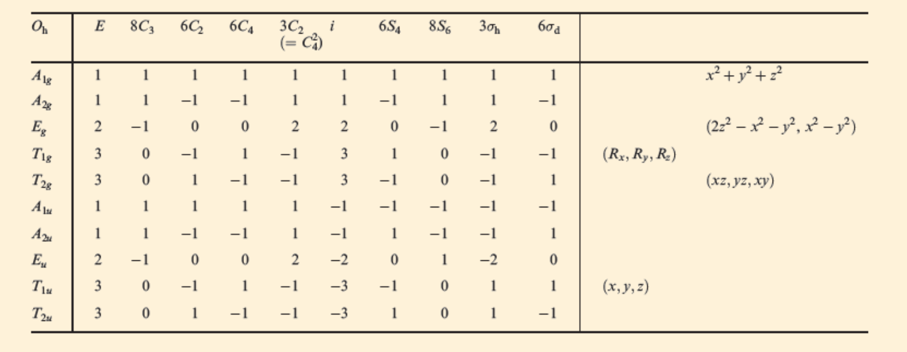

O_h	E	$8C_3$	$6C_2$	$6C_4$	$3C_2$ $(=C_4^2)$	i	$6S_4$	$8S_6$	$3\sigma_h$	$6\sigma_d$		
A_{1g}	1	1	1	1	1	1	1	1	1	1		$x^2+y^2+z^2$
A_{2g}	1	1	−1	−1	1	1	−1	1	1	−1		
E_g	2	−1	0	0	2	2	0	−1	2	0		$(2z^2-x^2-y^2, x^2-y^2)$
T_{1g}	3	0	−1	1	−1	3	1	0	−1	−1	(R_x, R_y, R_z)	
T_{2g}	3	0	1	−1	−1	3	−1	0	−1	1		(xz, yz, xy)
A_{1u}	1	1	1	1	1	−1	−1	−1	−1	−1		
A_{2u}	1	1	−1	−1	1	−1	1	−1	−1	1		
E_u	2	−1	0	0	2	−2	0	1	−2	0		
T_{1u}	3	0	−1	1	−1	−3	−1	0	1	1	(x, y, z)	
T_{2u}	3	0	1	−1	−1	−3	1	0	1	−1		

d_{z^2} and $d_{x^2-y^2}$ orbitals have e_g symmetry,
d_{xy}, d_{yz} and d_{xz} orbitals possess t_{2g} symmetry

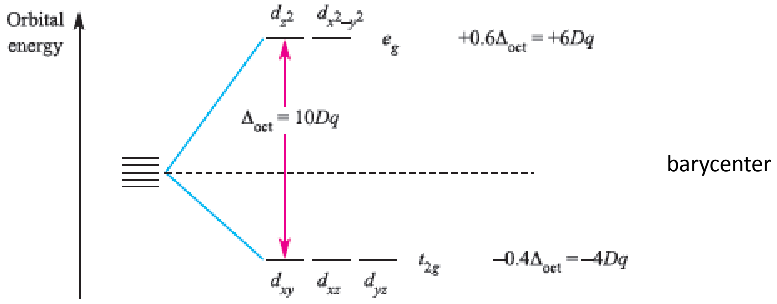

- The energy separation between them is Δ_{oct} ('delta oct') or 10D*q*.
- The overall stabilization of the t_{2g} orbitals equals the overall destabilization of the e_g set.

The magnitude of Δoct is determined by the strength of the crystal field, the two extremes being called ***weak field*** and ***strong field***

$$\Delta_{oct}(\text{weak field}) < \Delta_{oct}(\text{strong field})$$

in principle at least, values of Δ_{oct} can be evaluated from electronic spectroscopic data

Consider the ***d*¹** complex $[Ti(OH_2)_6]^{3+}$, for which the ground state is represented by diagram 21.2 or the notation $\boldsymbol{t_{2g}^{1} e_g^{0}}$.

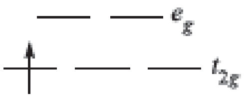

(21.2)

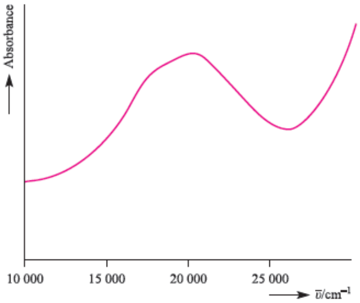

λ_{max} =20 300 cm^{-1} corresponding to an energy change of 243 kJ mol^{-1}. (1 cm^{-1} =11.96 $\times 10^3$ kJ mol^{-1}.)

value of λ_{max} gives a measure of Δ_{oct}.

Factors governing the magnitude of Δ_{oct}

- identity and oxidation state of the metal ion
- the nature of the ligands

For octahedral complexes, Δ_{oct} increases along the following ***spectrochemical*** series of ligands

$$\mathrm{I^- < Br^- < [NCS]^- < Cl^- < F^- < [OH]^- < [ox]^{2-}}$$
$$\mathrm{\approx H_2O < [NCS]^- < NH_3 < en < bpy < phen < [CN]^- \approx CO}$$

weak field ligands ⟶ strong field ligands increasing Δ_{oct}

The ***spectrochemical*** series is reasonably ***general***. Ligands with the same donor atoms are close together in the series.

The complexes of Cr(III) listed in Table 21.2 illustrate the effects of different ligand field strengths for a given **M^{n+}** ion;

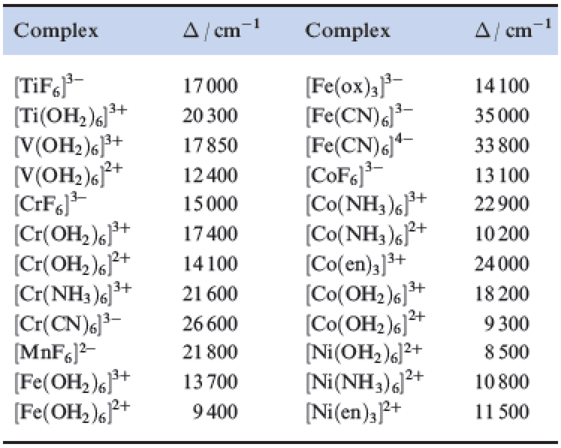

Complex	Δ / cm^{-1}	Complex	Δ / cm^{-1}
$[TiF_6]^{3-}$	17 000	$[Fe(ox)_3]^{3-}$	14 100
$[Ti(OH_2)_6]^{3+}$	20 300	$[Fe(CN)_6]^{3-}$	35 000
$[V(OH_2)_6]^{3+}$	17 850	$[Fe(CN)_6]^{4-}$	33 800
$[V(OH_2)_6]^{2+}$	12 400	$[CoF_6]^{3-}$	13 100
$[CrF_6]^{3-}$	15 000	$[Co(NH_3)_6]^{3+}$	22 900
$[Cr(OH_2)_6]^{3+}$	17 400	$[Co(NH_3)_6]^{2+}$	10 200
$[Cr(OH_2)_6]^{2+}$	14 100	$[Co(en)_3]^{3+}$	24 000
$[Cr(NH_3)_6]^{3+}$	21 600	$[Co(OH_2)_6]^{3+}$	18 200
$[Cr(CN)_6]^{3-}$	26 600	$[Co(OH_2)_6]^{2+}$	9 300
$[MnF_6]^{2-}$	21 800	$[Ni(OH_2)_6]^{2+}$	8 500
$[Fe(OH_2)_6]^{3+}$	13 700	$[Ni(NH_3)_6]^{2+}$	10 800
$[Fe(OH_2)_6]^{2+}$	9 400	$[Ni(en)_3]^{2+}$	11 500

- the complexes of Fe(II) and Fe(III) in Table 21.2 illustrate that for a given ligand and a given metal, Δ_{oct} increases with increasing oxidation state
- where analogous complexes exist for a series of M^{n+} metals ions (constant n) in a triad, Δ_{oct} increases significantly down the triad

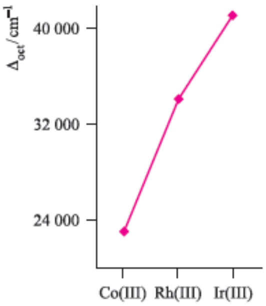

- for a given ligand and a given oxidation state, Δ_{oct} varies irregularly across the first row of the *d*-block

Metal ions can be placed in a ***spectrochemical*** series which is independent of the ligands:

$$\xrightarrow[\text{increasing field strength}]{\begin{array}{l}\text{Mn(II)} < \text{Ni(II)} < \text{Co(II)} < \text{Fe(III)} < \text{Cr(III)} < \text{Co(III)} \\ \quad < \text{Ru(III)} < \text{Mo(III)} < \text{Rh(III)} < \text{Pd(II)} < \text{Ir(III)} < \text{Pt(IV)}\end{array}}$$

Spectrochemical series are empirical generalizations and simple crystal field theory cannot account for the magnitudes of Δ_{oct} values.

Exchange energies

Consider two electrons in different orbitals. The repulsion between the electrons if they have anti-parallel spins is greater than if they have parallel spins, e.g. for a p^2 configuration:

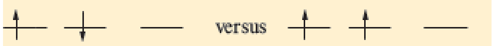

The difference in energy between these two configurations is the **exchange energy**, **K** i.e. this is the extra stability that the right-hand configuration has with respect to the left-hand one

$$\text{Exchange energy} = \sum \frac{N(N-1)}{2} K$$

where N = number of electrons with parallel spins.

Crystal field stabilization energy: high- and low-spin octahedral complexes

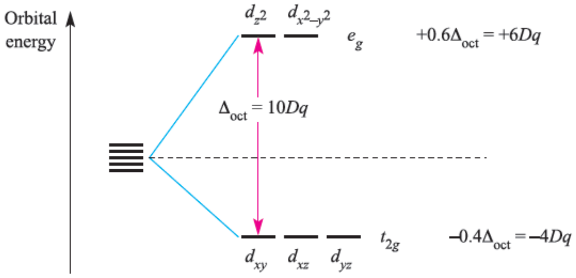

For a d1 system, the ground state corresponds to the configuration t_{2g}^1

With respect to the barycenter, there is a stabilization energy of **$-0.4\Delta_{oct}$** ***crystal field stabilization energy***, **CFSE**

For a **d²** ion, the ground state configuration is t_{2g}^2 and the CFSE = $-0.8\Delta_{oct}$.
A **d³** ion (t_{2g}^3) has a CFSE = $-1.2\Delta_{oct}$.

For a ground state *d*⁴ ion

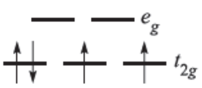

t_{2g}^4

low-spin arrangement

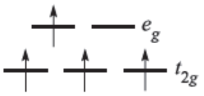

$t_{2g}^3 e_g^1$

high-spin arrangement

The preferred configuration is that with the lower energy

electron-pairing energy, **P**, which is the energy required to transform two electrons with parallel spin in different degenerate orbitals into spin-paired electrons in the same orbital.

- the loss in the exchange energy (see Box 1.8) which occurs upon pairing the electrons;
- the coulombic repulsion between the *spin-paired* electrons.

For a ground state *d*⁴ ion

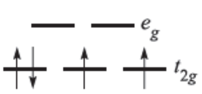

t_{2g}^{4}

low-spin

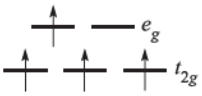

$t_{2g}^{3} e_g^{1}$

high-spin

CFSE consists of two terms:

$-1.6\Delta_{oct} + P$

$$\text{CFSE} = -(3 \times 0.4)\Delta_{\text{oct}} + 0.6\Delta_{\text{oct}} = -0.6\Delta_{\text{oct}}$$

d^n	High-spin = weak field		Low-spin = strong field	
	Electronic configuration	CFSE	Electronic configuration	CFSE
d^1	$t_{2g}{}^1e_g{}^0$	$-0.4\Delta_{oct}$		
d^2	$t_{2g}{}^2e_g{}^0$	$-0.8\Delta_{oct}$		
d^3	$t_{2g}{}^3e_g{}^0$	$-1.2\Delta_{oct}$		
d^4	$t_{2g}{}^3e_g{}^1$	$-0.6\Delta_{oct}$	$t_{2g}{}^4e_g{}^0$	$-1.6\Delta_{oct} + P$
d^5	$t_{2g}{}^3e_g{}^2$	0	$t_{2g}{}^5e_g{}^0$	$-2.0\Delta_{oct} + 2P$
d^6	$t_{2g}{}^4e_g{}^2$	$-0.4\Delta_{oct}$	$t_{2g}{}^6e_g{}^0$	$-2.4\Delta_{oct} + 2P$
d^7	$t_{2g}{}^5e_g{}^2$	$-0.8\Delta_{oct}$	$t_{2g}{}^6e_g{}^1$	$-1.8\Delta_{oct} + P$
d^8	$t_{2g}{}^6e_g{}^2$	$-1.2\Delta_{oct}$		
d^9	$t_{2g}{}^6e_g{}^3$	$-0.6\Delta_{oct}$		
d^{10}	$t_{2g}{}^6e_g{}^4$	0		

For high-spin: $\Delta_{oct} < P$

For low-spin: $\Delta_{oct} > P$

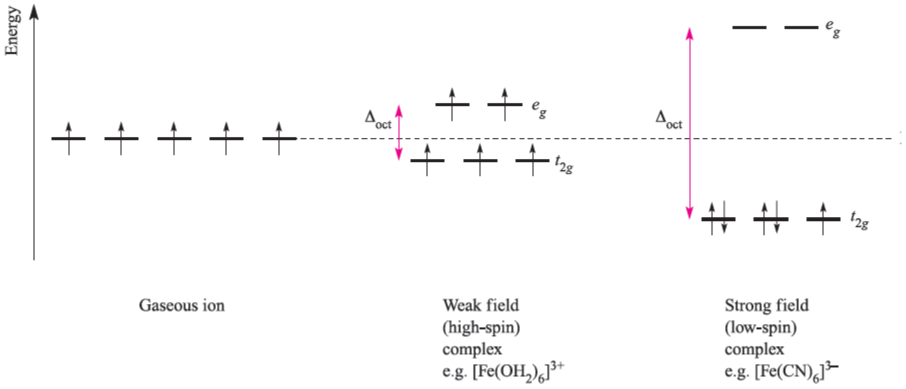

- **Strong field ligands** such as $[CN]^-$ favor the formation of ***low-spin*** complexes
- **weak field ligands** such as halides tend to favor ***high-spin*** complexes.

if we know from magnetic data that $[Co(OH_2)_6]^{3+}$ is **low-spin**, then from the spectrochemical series we can say that

$[Co(ox)_3]^{3-}$ and $[Co(CN)_6]^{3-}$ will be **low-spin**.

The only common **high-spin** cobalt(III) complex is $[CoF_6]^{3-}$.

Jahn-Teller distortions (*tetragonal distortions*).

Octahedral complexes of **d⁹** and high-spin **d⁴** ions are often distorted

two metal–ligand bonds (axial) are different lengths from the remaining four (equatorial).

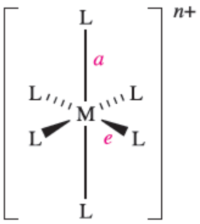

Bond length $a > e$

(21.5)

elongated octahedron

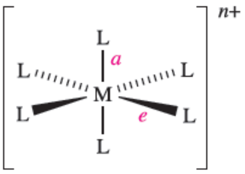

Bond length $a < e$

(21.6)

compressed octahedron

For a high-spin d^4 ion, one of the e_g orbitals contains one electron while the other is vacant.

If the singly occupied orbital is the d_{z^2} , most of the electron density in this orbital will be concentrated between the cation and the two ligands on the z axis.

Thus, there will be greater electrostatic repulsion associated with these ligands than with the other four and the complex suffers elongation

Conversely, occupation of the $d_{x^2-y^2}$ orbital would lead to elongation along the x and y axes as in structure

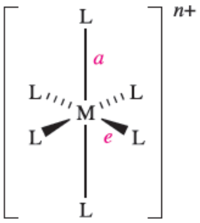

Bond length $a > e$

(21.5)

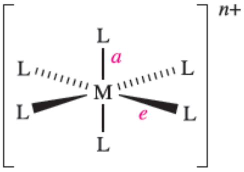

Bond length $a < e$

(21.6)

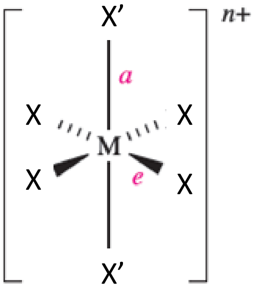

	Cu–X	Cu – X’
X= Cl	2.3	2.95
Br	2.4	3.18
F	1.93	2.27

The **Jahn–Teller theorem** states that any **non-linear** molecular system in a **degenerate electronic state** will be **unstable** and will undergo **distortion** to form a system of **lower symmetry** and **lower energy**, thereby removing the degeneracy.

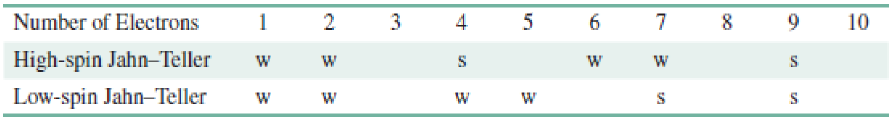

Number of Electrons	1	2	3	4	5	6	7	8	9	10
High-spin Jahn–Teller	w	w		s		w	w		s	
Low-spin Jahn–Teller	w	w		w	w		s		s	

w = weak Jahn–Teller effect expected (t_{2g} orbitals unevenly occupied);
s = strong Jahn–Teller effect expected (e_g orbitals unevenly occupied);
No entry = no Jahn–Teller effect expected.

The tetrahedral crystal field

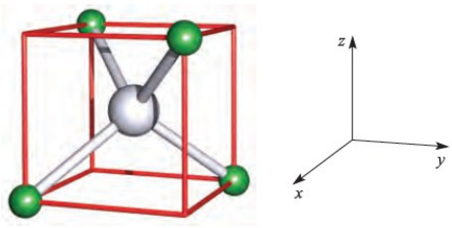

The relationship between a tetrahedral ML_4 complex and a cube

With the complex in this orientation, *none* of the metal ***d*** orbitals points exactly at the ligands, but the d_{xy}, d_{yz} and d_{xz} orbitals come nearer to doing so than the d_{z^2} and $d_{x^2-y^2}$ orbitals.

For a regular tetrahedron, the splitting of the ***d*** orbitals is inverted compared with that for a regular octahedral structure, and the energy difference (Δ_{tet}) is smaller.
If all other things are equal (and of course, they never are), the relative splittings Δ_{oct} and Δ_{tet} are related by equation

$$\Delta_{\text{tet}} = \tfrac{4}{9}\Delta_{\text{oct}} \approx \tfrac{1}{2}\Delta_{\text{oct}}$$

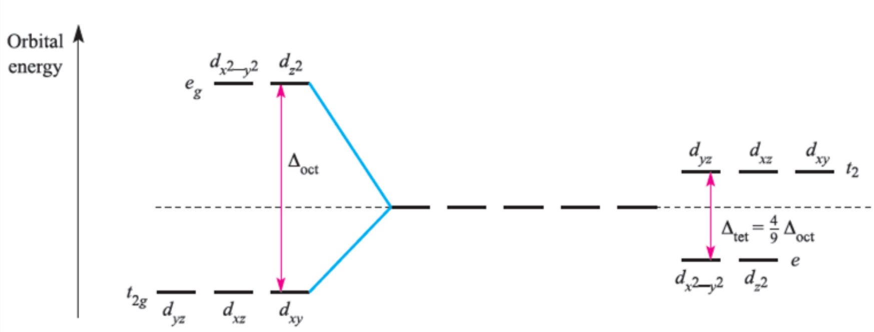

Since Δ_{tet} is significantly smaller than Δ_{oct}, tetrahedral complexes are high-spin.

Notation for electronic transitions

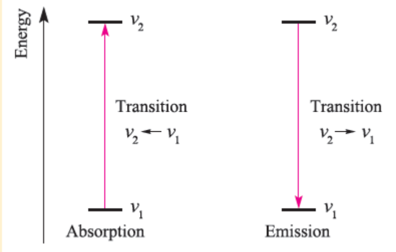

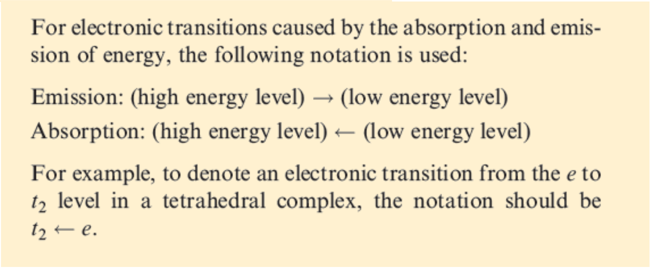

For electronic transitions caused by the absorption and emission of energy, the following notation is used:

Emission: (high energy level) ⟶ (low energy level)

Absorption: (high energy level) ⟵ (low energy level)

For example, to denote an electronic transition from the e to t_2 level in a tetrahedral complex, the notation should be $t_2 \leftarrow e$.

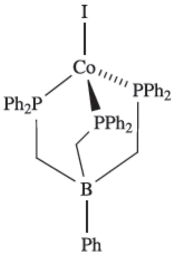

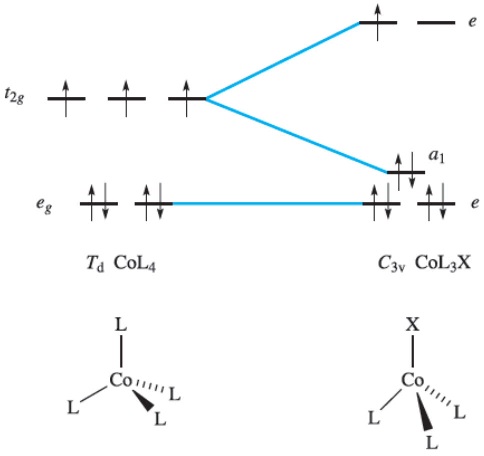

[$PhB(CH_2PPh_2)_3CoI$] is a rare example of a ***low-spin***, distorted tetrahedral complex. The tripodal tris(phosphine) is a strong-field ligand.

The square planar crystal field

A square planar arrangement of ligands can be formally derived from an octahedral array by removal of two trans ligands

If we remove the ligands lying along the z axis, then the d_{z^2} orbital is greatly stabilized; the energies of the d_{yz} and d_{xz} orbitals are also lowered

The fact that square planar d^8 complexes such as $[Ni(CN)_4]^{2-}$ are diamagnetic is a consequence of the relatively large energy difference between the d_{xy} and $d_{x^2-y^2}$ orbitals.

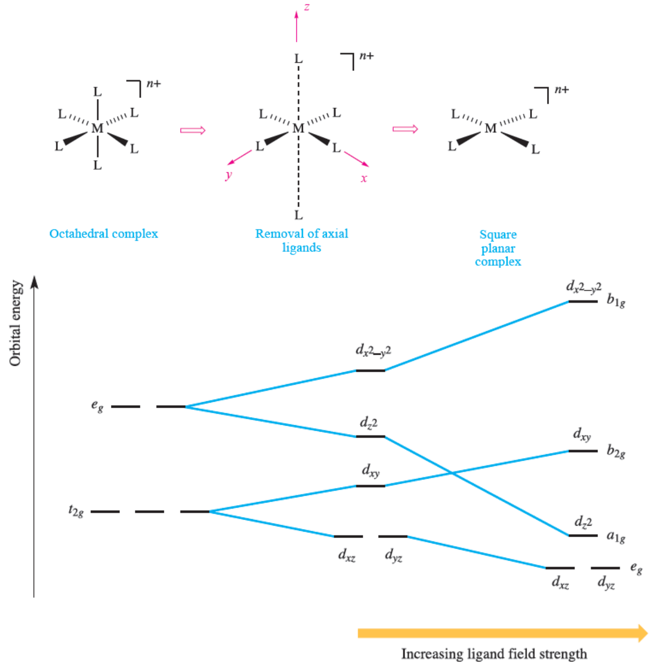

Worked example 21.1

The d^8 complexes $[Ni(CN)_4]^{2-}$ and $[Ni(Cl)_4]^{2-}$ are square planar and tetrahedral respectively. Will these complexes be paramagnetic or diamagnetic?

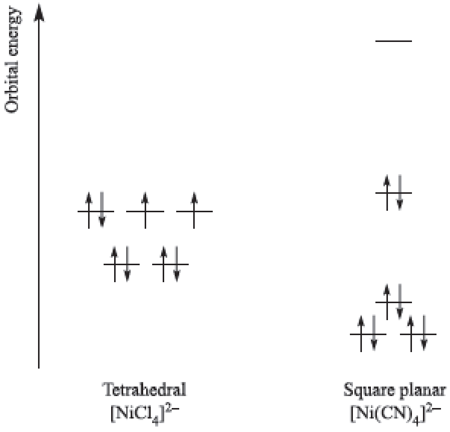

Other crystal fields

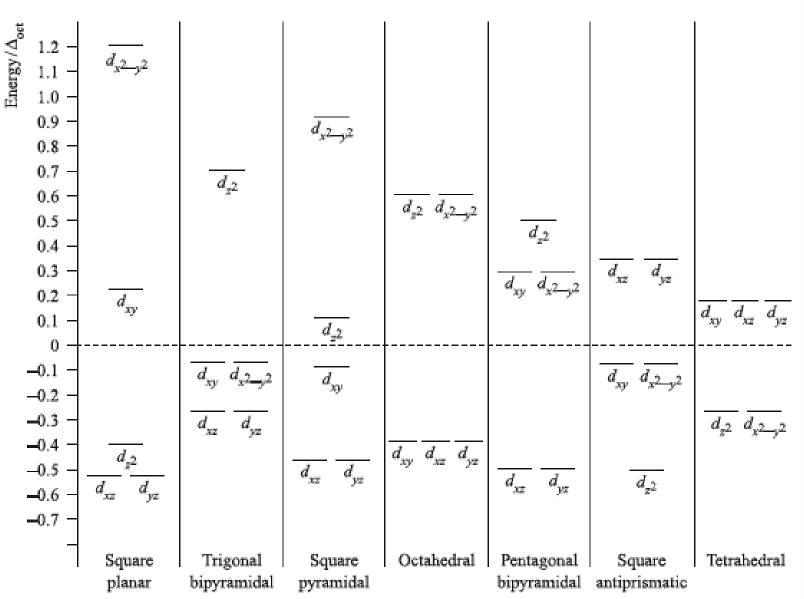

Crystal field theory: uses and limitations

Crystal field theory can bring together structures, magnetic properties and electronic properties.

Crystal field theory provides no explanation as to why particular ligands are placed where they are in the ***spectrochemical*** series.

21.4 Molecular orbital theory: octahedral complexes

molecular orbital model considers covalent interactions between the metal center and ligands

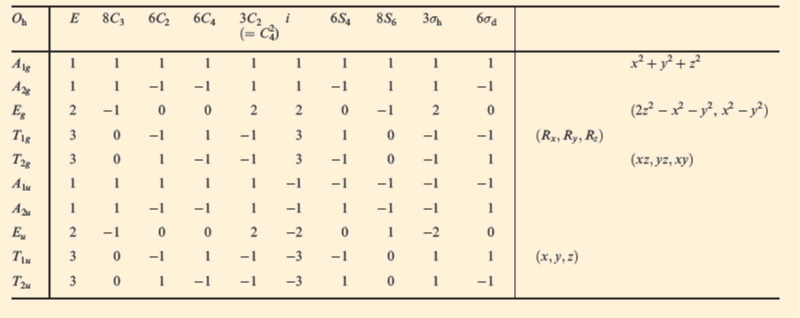

O_h	E	$8C_3$	$6C_2$	$6C_4$	$3C_2$ $(= C_4^2)$	i	$6S_4$	$8S_6$	$3\sigma_h$	$6\sigma_d$		
A_{1g}	1	1	1	1	1	1	1	1	1	1		$x^2 + y^2 + z^2$
A_{2g}	1	1	−1	−1	1	1	−1	1	1	−1		
E_g	2	−1	0	0	2	2	0	−1	2	0		$(2z^2 - x^2 - y^2, x^2 - y^2)$
T_{1g}	3	0	−1	1	−1	3	1	0	−1	−1	(R_x, R_y, R_z)	
T_{2g}	3	0	1	−1	−1	3	−1	0	−1	1		(xz, yz, xy)
A_{1u}	1	1	1	1	1	−1	−1	−1	−1	−1		
A_{2u}	1	1	−1	−1	1	−1	1	−1	−1	1		
E_u	2	−1	0	0	2	−2	0	1	−2	0		
T_{1u}	3	0	−1	1	−1	−3	−1	0	1	1	(x, y, z)	
T_{2u}	3	0	1	−1	−1	−3	1	0	1	−1		

The O_h character table is used to assign symmetries to the orbitals
on atom X, and to the ligand group orbitals. The MO diagram is then constructed by allowing interactions between
orbitals of the same symmetry. Only ligand group orbitals that can be classified within the point group of the whole molecule are allowed.

By following the procedures that in Chapter 5

An **MO diagram** can be constructed to describe the bonding in an $\boldsymbol{O_h}$ ML_6^{n+} complex.
For a first row metal, the valence shell atomic orbitals are **3*d***, **4*s*** and **4*p***.

Under O_h symmetry (see Appendix 3)

- the ***s*** orbital has $\mathbf{a_{1g}}$ symmetry,
- the ***p*** orbitals are degenerate with $\boldsymbol{t_{1u}}$ symmetry,
- the ***d*** orbitals split into two sets with $\mathbf{e_g}$ (d_{z^2} and $d_{x^2-y^2}$ orbitals) and $\mathbf{t_{2g}}$ (d_{xy}, d_{yz} and d_{xz} orbitals) symmetries
- Each ligand, L, provides **one orbital** and derivation of the ligand group orbitals (LGOs) for the $\boldsymbol{O_h}$ $\mathbf{L_6}$ fragment is analogous to those for the F_6 fragment in SF_6 see Figure **5.27**, equations 5.26–5.31 and accompanying text.

These LGOs have $\mathbf{a_{1g}}$, $\mathbf{t_{1u}}$ and $\mathbf{e_g}$ symmetries (Figure 21.12). Symmetry matching between metal orbitals and LGOs allows the construction of the MO diagram shown in Figure 21.13.

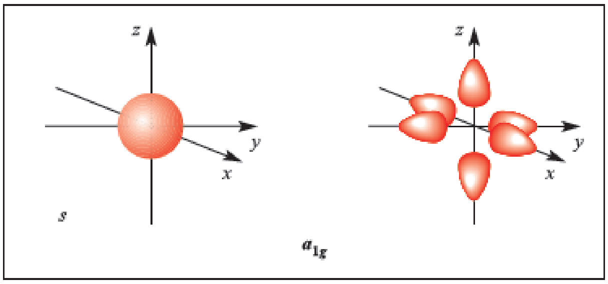

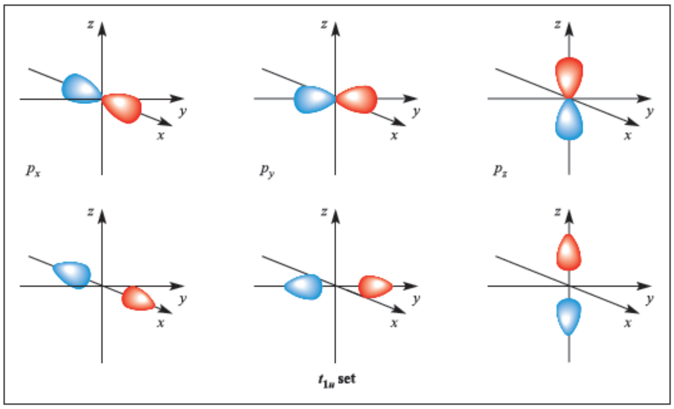

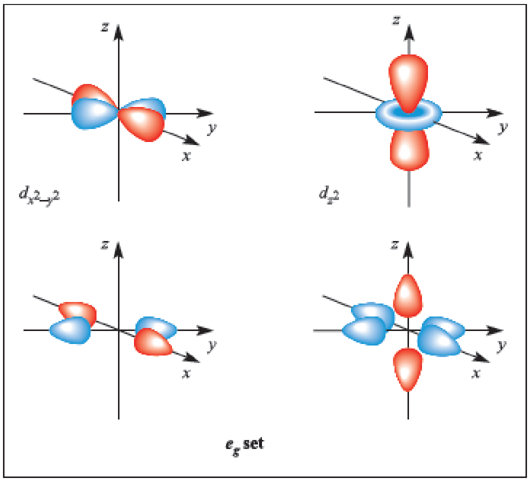

Metal atomic orbitals ***s***, p_x, p_y, p_z, $d_{x^2-y^2}$, d_{z^2} matched by symmetry with ligand group orbitals for an octahedral O_h complex with only -bonding.

- Combinations of the metal and ligand orbitals generate six bonding and six antibonding molecular orbitals.
- The metal $\mathbf{d}_{xy}$, $\mathbf{d}_{yz}$ and $\mathbf{d}_{xz}$ atomic orbitals have $\mathbf{t}_{2g}$ symmetry and are **non-bonding**
- The overlap between the ligand and metal ***s*** and ***p*** orbitals is greater than that involving the metal ***d*** orbitals, and so the $\mathbf{a}_{1g}$ and $\mathbf{t}_{1u}$ MOs are stabilized to a greater extent than the $\mathbf{e}_{g}$ MOs.
- In an octahedral complex with no ***π-bonding***, the energy difference between the $\mathbf{t}_{2g}$ and $\mathbf{e}_{g}$ levels corresponds to Δ_{oct} in crystal field theory (Figure 21.13).

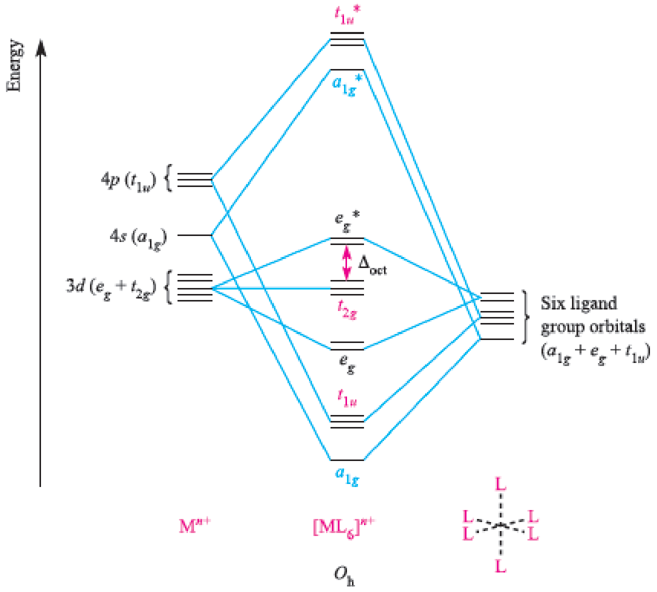

We are able to describe the bonding in a range of octahedral-bonded complexes.

in low-spin $[Co(NH_3)_6]^{3+}$, 18 electrons (six from Co^{3+} and two from each ligand) occupy the $\mathbf{a_{1g}}$, $\mathbf{t_{1u}}$, $\mathbf{e_g}$ and $\mathbf{t_{2g}}$ MOs

in high-spin CoF_6^{3-}, 18 electrons are available, 12 occupying the $\mathbf{a_{1g}}$, $\mathbf{t_{1u}}$ and $\mathbf{e_g}$ MOs, four the $\mathbf{t_{2g}}$ level, and two the $\mathbf{e_g}$ level.

Complexes with metal-ligand π-bonding

The metal d_{xy}, d_{yz} and d_{xz} atomic orbitals (the t_{2g} set) are nonbonding in an ML_6^{n+}, σ-bonded complex (Figure 21.13) and these orbitals may overlap with ligand orbitals of the c

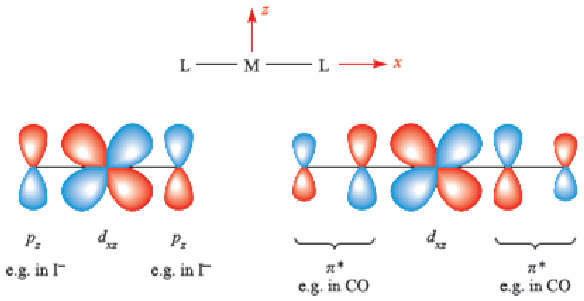

π-donor ligand **π-acceptor ligand**

A **π-donor** ligand **donates** electrons to the metal center in an interaction that involves a ***filled ligand orbital*** and an ***empty metal orbital***

A **π-acceptor** ligand **accepts** electrons from the metal center in an interaction that involves a ***filled metal orbital*** and an ***empty ligand orbital***.

π-Donor ligands include Cl^-, Br^- and I^- and the metal– ligand π-interaction involves transfer of electrons from filled ligand ***p*** orbitals to the metal center

Examples of π-acceptor ligands are **CO**, **N_2**, **NO** and **alkenes**, and the metal–ligand π-bonds arise from the ***back-donation*** of electrons from the metal center to vacant ***antibonding*** orbitals on the ligand

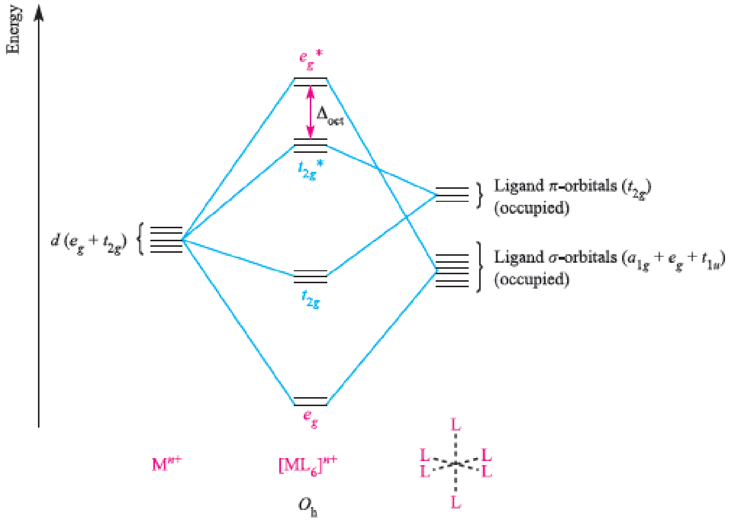

Approximate partial MO diagrams for metal–ligand π-bonding in an octahedral complex with π-donor ligands

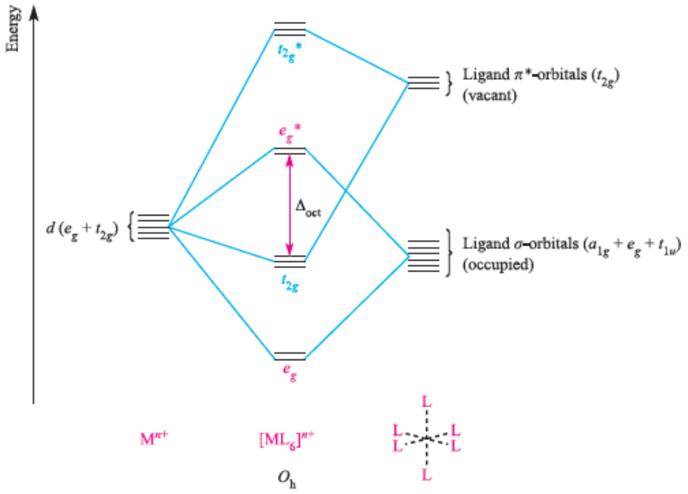

Approximate partial MO diagrams for metal–ligand π-bonding in an octahedral complex with π-acceptor ligands

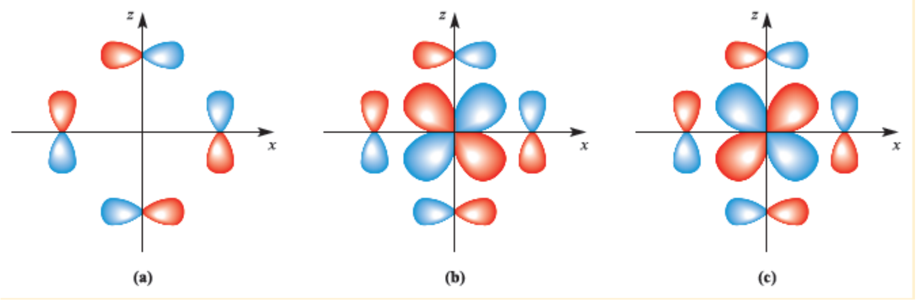

a. ligand group orbital (LGO) comprising the p_z orbitals of two ligands and the p_x orbitals of the other two.

Diagram (b) shows how the LGO in (a) combines with the metal d_{xz} orbital to give a bonding MO, while (c) shows the ***antibonding*** combination.

- Δ_{oct} decreases in going from a σ-complex to one containing π-donor ligands;
- for a complex with π-donor ligands, increased π-donation stabilizes the t_{2g} level and destabilizes the t_{2g}^*, thus decreasing Δ_{oct};
- Δ_{oct} values are relatively large for complexes containing π-acceptor ligands, and such complexes are likely to be **low-spin**
- for a complex with π-acceptor ligands, increased π-acceptance stabilizes the t_{2g} level, increasing Δ_{oct}.

The above points are consistent with the positions of the ligands in the ***spectrochemical*** series;

- π-donors such as I^- and Br^- are weak-field,
- while π-acceptor ligands such as CO and $[CN]^-$ are strong-field ligands.

Six π-donor ligands provide 18 electrons (12 σ- and 6 π-electrons) and these can notionally be considered to occupy the a_{1g}, t_{1u}, e_g and t_{2g} orbitals of the complex.

The occupancy of the t_{2g}^* and e_g^* levels corresponds to the number of valence electrons of the metal ion.

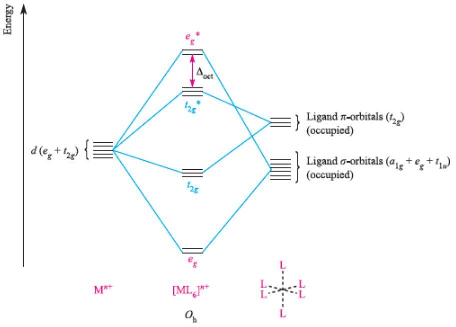

Six π-acceptor ligands provide 12 electrons (i.e. 12 -electrons since the π-ligand orbitals are empty) and, formally, we can place these in the a_{1g}, t_{1u} and e_g orbitals of the complex.
The number of electrons supplied by the metal center then corresponds to the occupancy of the t_{2g} and e_g* levels. Since occupying ***antibonding*** MOs lowers the metal–ligand bond order

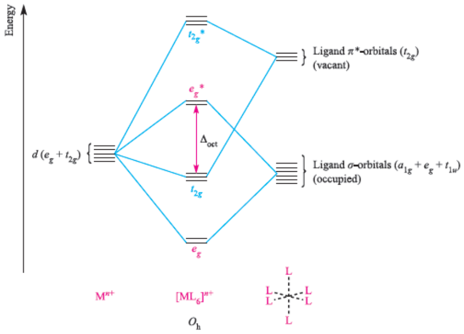

octahedral complexes with π-accepting ligands will not be favored for metal centers with d^7, d^8, d^9 or d^{10} configurations.

d-block metal organometallic and related complexes tend to obey the ***effective atomic number rule*** or **18-electron rule**.

A low oxidation state organometallic complex contains **π-acceptor** ligands and the metal center tends to acquire 18 electrons in its valence shell (the 18-electron rule), thus filling the valence orbitals, e.g. Cr in $Cr(CO)_6$, Fe in $Fe(CO)_5$, and Ni in $Ni(CO)_4$.

NO as a 3-electron donor:

M–N–O $\angle$165–180^{o}) and short M–N and N–O bonds indicating multiple bond character

N atom taken to be ***sp*** hybridized

NO as a 1-electron donor:

bent MNO group (observed range $\angle$ MNO ≈ 120–140^{o}), and NO bond length typical of a double b

N atom considered as sp^2 hybridized

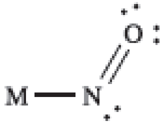

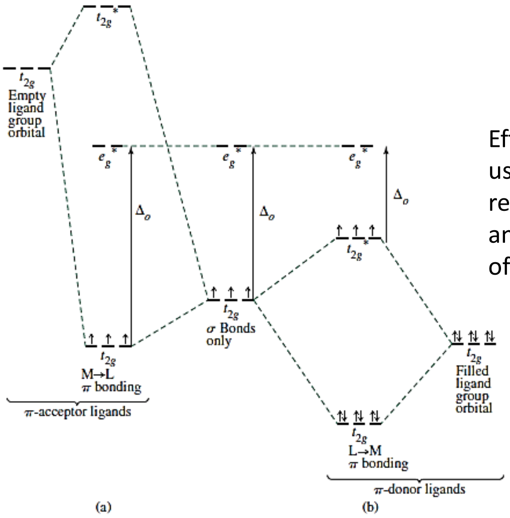

Effects of π-Bonding on Δ_{oct} using a d^3 Ion. Figure(a) is representative of $[Cr(CN)_6]^{3-}$ and Figure (b) is representative of $[CrF_6]^{3-}$.

Extensive ligand-to-metal π-bonding usually favors **high-spin** configurations, and metal-to-ligand π-bonding favors **low-spin** configurations, consistent with the effect on Δ_{oct} caused by these interactions.

21.6 Describing electrons in *multielectron* systems

How we describe the interactions between electrons in ***multielectron*** systems.

In crystal field theory, we have considered repulsions between ***d***-electrons and **ligand** electrons, but have ignored interactions between ***d***-electrons on the metal center.

simple electron configurations such as **$2s^2 2p^1$** or **$4s^2 3d^2$** do not uniquely define the arrangement of the electrons.

Quantum numbers L and M_L for ***multielectron*** species

For any system containing more than one electron, the energy of an electron with principal quantum number *n* depends on the value of *l*

$$\text{Orbital angular momentum} = \left(\sqrt{l(l+1)}\right)\frac{h}{2\pi}$$

Quantum numbers for electrons	***Quantum numbers for many-electron atoms***
l: orbital angular momentum quantum number (0, 1, … *n*–1 where 0=*s*, 1=*p*, 2=*d*, 3=*f*	***L***: orbital angular momentum quantum number e.g., for 2e⁻: $L = (l_1+l_2), (l_1+l_2-1), (l_1+l_2-2), \ldots, \vert l_1-l_2 \vert$ 0 = *S*, 1 = *P*, 2 = *D*, 3 = *F*, 4 = *G*
m_l: orbital magnetic quantum number $(l, l-1, \ldots, 0, \ldots, -l)$	M_L: orbital magnetic quantum number (Σm_l) $L, (L-1) \ldots 0 \ldots -(L-1), -L$. **2*L*+1** possible values If we can find all possible values of $\mathbf{M_L}$ for a multi-electron species, we can determine the value of **L** for the system.
s: electron spin quantum number (**1/2**)	***S***: total spin quantum number $S = s_1+s_2, s_1+s_2-1, \ldots, \vert s_1-s_2 \vert$ ***S*** = 0 singlet, S = 1 doublet, S = 2 triplet S = 1/2, 3/2, 5/2 … for an odd number of electrons S = 0, 1, 2 … for an even number of electrons .
m_s: spin magnetic quantum number (+1/2, –1/2)	M_S: spin magnetic quantum number (Σm_s) 2***S***+1 possible values M_S : $S, (S-1), \ldots -(S-1), -S$
	J: total angular quantum number $J = L+S, L+S-1, \ldots, \vert L-S \vert$

Microstates and term symbols

With sets of quantum numbers in hand, the electronic states (***microstates***) that are possible for a given electronic configuration can be determined.

table of microstates

- no two electrons may possess the same set of quantum numbers (the Pauli exclusion principle);
- only unique microstates may be included.

- ***Multiplicity (2S +1****)* *describes the number of possible orientations of total spin angular momentum where S is the resultant spin quantum number (1/2 x # unpaired electrons)*

- ***Resultant Angular Momentum (L)*** *describes the coupling of the orbital angular momenta of each electron (add the* m_L *values for each electron)*

- ***Total Angular Momentum (J)*** *combines orbital angular momentum and intrinsic angular momentum (i.e., spin).*

- *To Assign* ***J*** *Value:*
  if less than half of the subshell is occupied, take the minimum value ***J = | L – S |*** *;*
  if more than half-filled, take the maximum value ***J = L + S****;*
  if the subshell is half-filled, ***L = 0*** *and then* ***J = S****.*

Case 1: *ns*^{2} configuration

- first microstate: $l = 0$, $m_l = 0$, $m_s = +1/2$; $l = 0$, $m_l = 0$, $m_s = -1/2$
- second microstate: $l = 0$, $m_l = 0$, $m_s = -1/2$; $l = 0$, $m_l = 0$, $m_s = +1/2$

First electron: $m_l = 0$	Second electron: $m_l = 0$	$M_L = \Sigma m_l$	$M_S = \Sigma m_s$	
↑ ↓	↓ ↑	0	0	$L = 0, S = 0$

- The microstates are identical (the electrons have simply been switched around) and so one microstate is discounted.
- Hence, for the ***ns*²** configuration, only ***one microstate*** is possible.
- The values of $\mathbf{M_S}$ and $\mathbf{M_L}$ are obtained by reading across the table.
- The result in Table 21.4 is represented as a term symbol which has the form $^{(2S+1)}\mathbf{L}$, where **(2S + 1)** is called the ***multiplicity*** of the term:

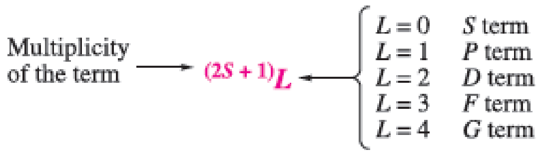

- Terms for which (2S + 1) = 1, 2, 3, 4 ... (corresponding to S = 0, 1/2, 1, 3/2 ...) are called singlet, doublet, triplet, quartet ... terms, respectively.
- Hence, the ns^2 configuration in Table 21.4 corresponds to a ^1S term (a '**singlet S term**').

Case 2: $ns^1n's^1$ configuration

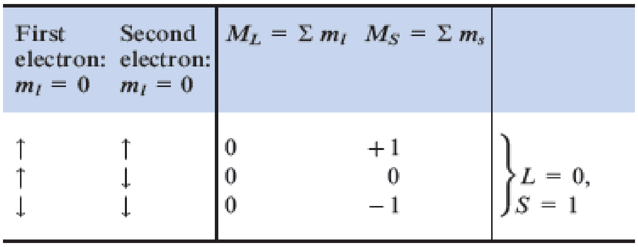

First electron: $m_l = 0$	Second electron: $m_l = 0$	$M_L = \Sigma m_l$	$M_S = \Sigma m_s$	
↑	↑	0	+1	$L = 0$, $S = 1$
↑	↓	0	0	
↓	↓	0	−1	

^3S term (a 'triplet S term').

Values of M_S and M_L are obtained by reading across the table. Values of L and S are obtained by fitting the values of M_S and M_L to the series:

M_L : L, (L – 1) ... 0, ... –(L – 1), –L
M_S : S, (S – 1) ... –(S – 1), –S

The quantum numbers *J* and M_J

interaction between the total angular orbital momentum, L, and the total spin angular momentum, S.

J = (L +S), (L+S – 1) …… |L – S|

It follows that there are **(2S + 1)** possible values of J for **S < L**, and **(2L+1)** possible values for **L < S**.

Allowed values of $\mathbf{M_J}$: *J*, (*J* – 1) ... –(*J* – 1), –*J*

full term symbols which include information about S, L and J

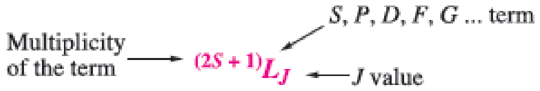

A term symbol $^3P_0$ ('triplet P zero') signifies a term with L = 1, (2S+1) = 3 (i.e. S = 1), and J = 0.

Different values of J denote different levels within the term, i.e. $^{(2S+1)}L_{J1}$, $^{(2S+1)}L_{J2}$ ... , for example·

The degeneracy of any ***J*** level is (2*J* + 1)

The ***J*** levels have different energies

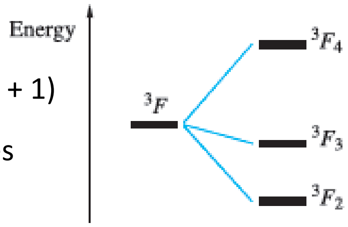

Ground states of elements with Z = 1-10

only electrons in open (incompletely filled) shells (e.g. ns^1, np^2, nd^4) contribute to the term symbol.

Follow these 'rules' when constructing a table of microstates:

1. Write down the electron configuration (e.g. d^2).
2. Ignore closed shell configurations (e.g. ns^2, np^6, nd^{10}) as these will always give a $^1S_0$ term. This is totally symmetric and makes no contribution to the angular momentum.
3. Determine the number of microstates: for x electrons in a sub-level of (2*l* + 1) orbitals, this is given by:

$$\frac{\{2(2l+1)\}!}{x!\{2(2l+1)-x\}!}$$

4. Tabulate microstates by ml and ms, and sum to give M_L and M_S on each row. Check that the number of microstates in the table is the same as that expected from rule (3).
5. Collect the microstates into groups based on values of M_L.

Hydrogen (Z=1)

$1s^1$ ($l = 0$)

$$\text{Number of microstates} = \frac{\{2(2l+1)\}!}{x!\{2(2l+1)-x\}!} = \frac{2!}{1! \times 1!} = 2$$

	m_l	M_L	M_S
	0		
Up (m_s=+1/2)	↑	0	+1/2
down(m_s=−1/2)	↓	0	−1/2

$$\begin{array}{cc|cc} & & \multicolumn{2}{c}{M_S} \\ & & 1/2 & -1/2 \\ \hline M_L & 0 & 1 & 1 \end{array}$$

$^2S_{1/2}$

Helium (Z=2)

$m_l = 0$	$m_l = 0$	$M_L = \Sigma m_l$	$M_S = \Sigma m_s$	
↑	↓	0	0	$\}L = 0, S = 0$

$$\begin{array}{cc|c} & & M_S \\ & & 0 \\ \hline M_L & 0 & 1 \end{array}$$

Since M_L=0 and M_S=0, it follows that L=0 and S=0.

The only value of J is 0, and so the term symbol is $^1S_0$.

Boron (Z=5) ($1s^2 2s^2 2p^1$)

p^1

$$\text{Number of microstates} = \frac{\{2(2l+1)\}!}{x!\{2(2l+1)-x\}!} = \frac{6!}{1! \times 5!} = 6$$

m_l			M_L	M_S
+1	0	-1		
↑			1	+1/2
	↑		0	+1/2
		↑	-1	+1/2
↓			1	−1/2
	↓		0	−1/2
		↓	-1	−1/2

M_S

		1/2	−1/2
	+1	1	1
M_L	0	1	1
	-1	1	1

L=1 and S=1/2.
J = 3/2 and 1/2.

The term symbol for boron may be ${}^2\boldsymbol{P}_{3/2}$ or ${}^2\boldsymbol{P}_{1/2}$.

Carbon (Z=6) $1s^2 2s^2 2p^2$

$2p^2$

$$\text{Number of microstates} = \frac{\{2(2l+1)\}!}{x!\{2(2l+1)-x\}!} = \frac{6!}{2! \times 4!} = 15$$

m_l			M_L	M_S
+1	0	-1		
↑	↑		1	+1
↑		↑	0	+1
	↑	↑	–1	+1
↓	↓		1	–1
↓		↓	0	–1
	↓	↓	–1	–1
↑	↓		1	0
↑		↓	0	0
	↑	↓	–1	0
↓	↑		1	0
↓		↑	0	0
	↓	↑	–1	0
↓↑			2	0
	↓↑		0	0
		↓↑	–2	0

M_S

		+1	0	–1
	+2		1	
M_L	+1	1	2	1
	0	1	3	1
	-1	1	2	1
	-2		1	

M_L \ M_S	+1	0	−1
+2		1	
+1	1	2	1
0	1	3	1
-1	1	2	1
-2		1	

M_L \ M_S	0
+2	1
+1	1
0	1
-1	1
-2	1

L=2, S=0
J = 2.

$^1D_2$

M_L \ M_S	+1	0	−1
+1	1	1	1
0	1	1	1
-1	1	1	1

L=1, S=1
J = 2, 1, 0.

$^3P_2$, $^3P_1$ and $^3P_0$

M_L \ M_S	0
0	1

L=0, S=0
and J = 0.

$^1S_0$

For the relative energies of terms for a given electronic configuration: **(Hund's rules)**

1. The term with the highest spin multiplicity has the lowest energy.

2. If two or more terms have the same multiplicity (e.g. ^{3}F and ^{3}P), the term having the highest value of L has the lowest energy (e.g. ^{3}F is lower than ^{3}P).

3. For terms having the same multiplicity and the same values of L (e.g. $^3P_0$ and $^3P_1$),

- level with the **lowest value** of ***J*** is the lowest in energy if the sub-level is **less than** half-filled (e.g. p^2),
- level with the **highest value** of ***J*** is the more stable if the sub-level is **more than** half-filled (e.g. p^4).
- If the level is **half-filled** with maximum spin multiplicity (e.g. p^3 with ***S***=3/2), *L* must be zero, and *J*=*S*.

For p^2

The predicted energy ordering (from the rules above) is

$\mathbf{{}^3P_0 < {}^3P_1 < {}^3P_2 < {}^1D_2 < {}^1S_0}$,

and the ground state is the $^3P_0$ term.

Hence, the terms arising from the np^4 and np^2 configurations are the same. Similarly, np^5 is equivalent to np^1. This ***positive hole concept*** is very useful and we shall later extend it to n*d* configurations.

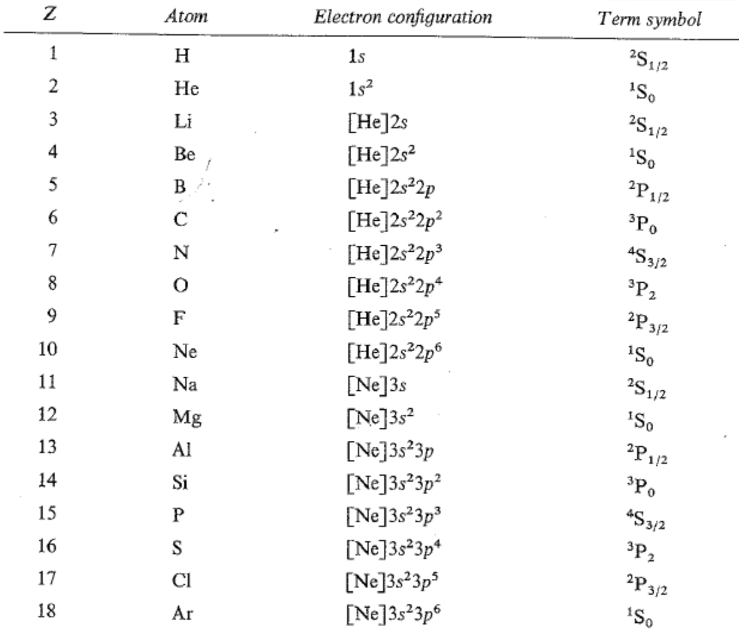

Z	*Atom*	*Electron configuration*	*Term symbol*
1	H	$1s$	$^2S_{1/2}$
2	He	$1s^2$	$^1S_0$
3	Li	$[He]2s$	$^2S_{1/2}$
4	Be	$[He]2s^2$	$^1S_0$
5	B	$[He]2s^22p$	$^2P_{1/2}$
6	C	$[He]2s^22p^2$	$^3P_0$
7	N	$[He]2s^22p^3$	$^4S_{3/2}$
8	O	$[He]2s^22p^4$	$^3P_2$
9	F	$[He]2s^22p^5$	$^2P_{3/2}$
10	Ne	$[He]2s^22p^6$	$^1S_0$
11	Na	$[Ne]3s$	$^2S_{1/2}$
12	Mg	$[Ne]3s^2$	$^1S_0$
13	Al	$[Ne]3s^23p$	$^2P_{1/2}$
14	Si	$[Ne]3s^23p^2$	$^3P_0$
15	P	$[Ne]3s^23p^3$	$^4S_{3/2}$
16	S	$[Ne]3s^23p^4$	$^3P_2$
17	Cl	$[Ne]3s^23p^5$	$^2P_{3/2}$
18	Ar	$[Ne]3s^23p^6$	$^1S_0$

The d^2 configuration

m_l					M_L	M_S
2	**1**	**0**	**-1**	**-2**		
↑	↑				3	1
↑		↑			2	1
↑			↑		1	1
↑				↑	0	1
	↑	↑			1	1
	↑		↑		0	1
	↑			↑	-1	1
		↑	↑		-1	1
		↑		↑	-2	1
			↑	↑	-3	1
↓	↓				3	–1
↓		↓			2	-1
↓			↓		1	-1
↓				↓	0	-1
	↓	↓			1	-1
	↓		↓		0	-1
	↓			↓	-1	-1
		↓	↓		-1	-1
		↓		↓	-2	-1
			↓	↓	-3	-1
↑	↓				3	0
↑		↓			2	0
↑			↓		1	0
↑				↓	0	0
	↑	↓			1	0
	↑		↓		0	0
	↑			↓	-1	0
		↑	↓		-1	0
		↑		↓	-2	0
			↑	↓	-3	0
↓	↑				3	0
↓		↑			2	0
↓			↑		1	0
↓				↑	0	0
	↓	↑			1	0
	↓		↑		0	0
	↓			↑	-1	0
		↓	↑		-1	0
		↓		↑	-2	0
			↓	↑	-3	0
↓↑					4	0
	↓↑				2	0
		↓↑			0	0
			↓↑		-2	0
				↓↑	-4	0

		Ms		
		+1	0	-1
M_L	4		1	
	3	1	2	1
	2	1	3	1
	1	2	4	2
	0	2	5	2
	-1	2	4	2
	-2	1	3	1
	-3	1	2	1
	-4		1	

	Ms
	0
4	1
3	1
2	1
1	1
0	1
-1	1
-2	1
-3	1
-4	1

S=0

L=4

J=4

$^1G_4$

		Ms	
	1	0	-1
3	1	1	1
2	1	1	1
1	1	1	1
0	1	1	1
-1	1	1	1
-2	1	1	1
-3	1	1	1

S=1

L=3

J=4, 3, 2

$^3F_4$ $^3F_3$ $^3F_2$

	Ms 0
2	1
1	1
0	1
-1	1
-2	1

S=0
L=2
J=2
$^1D_2$

		M_S 1	0	-1
	1	1	1	1
M_L	0	1	1	1
	-1	1	1	1

S=1
L=1
J=2 , 1, 0
$^3P_2$ $^3P_1$ $^3P_0$

		M_s 0
M_L	0	1

S=0
L=1
J=1
$^1S_0$

Hund's rules therefore predict the energy ordering of the terms for a ***d*²** configuration to be **$^3F < {}^3P < {}^1G < {}^1D < {}^1S$**.

The ***d*²** configuration is ***less than*** a half-filled level and so, if we include the ***J*** values, a more detailed description of the predicted ordering of the terms is **$^3F_2 < {}^3F_3 < {}^3F_4 < {}_3P_0 < {}^3P_1 < {}^3P_2 < {}^1G_4 < {}^1D_2 < {}^1S_0$**.

		m_l					M_L	M_S
	2	1	0	–1	–2			
	↑	↑					3	1

L=3 and S=1.
J = 4, 3, 2.

$^3F_2$ Ground state term

2d^3

	m_l						M_L	M_S
	2	1	0	–1	–2			
	↑	↑	↑				3	3/2

L=3 and S=3/2.
J = 9/2, 7/2, 5/2 , 3/2.

$^4F_{3/2}$ Ground state term

2p^4

m_l			M_L	M_S
+1	0	-1		
↑↓	↑	↑	1	1

L=1 and S=1.
J = 2, 1, 0.

$^3P_2$ Ground state term

21.7 Electronic spectra

Studies of electronic spectra of metal complexes provide information about structure and bonding.

Absorptions arise from transitions between electronic energy levels:

- transitions between metal-centred orbitals possessing d-character (‘d–d’ transitions);
- transitions between metal- and ligand-centred MOs which transfer charge from metal to ligand or ligand to metal (charge transfer bands).

Absorption bands in the electronic spectra of ***d***-block metal compounds are usually ***broad***.

Absorption bands are described in terms of ε_{max} corresponding to the absorption maximum A_{max} (Figure 21.16). The wavelength, λ_{max}, is usually given in nm, but the position of the absorption may also be reported in terms of wavenumbers, (cm^{-1}).

$$\varepsilon_{max} = \frac{A_{max}}{c \times \ell} \qquad (\varepsilon_{max} \text{ in dm}^3 \text{ mol}^{-1} \text{ cm}^{-1})$$

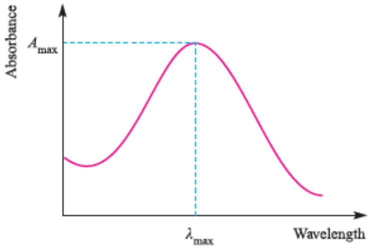

Values of ε_{max} range from close to zero (a very weak absorption) to >10 000 dm^3 mol^{-1} cm^{-1} (an intense absorption).

Some important points are that the electronic spectra of:

- d^1, d^4, d^6 and d^9 complexes consist of one broad absorption;
- d^2, d^3, d^7 and d^8 complexes consist of three broad absorptions
- d^5 complexes consist of a series of very weak, relatively sharp absorptions.

Charge transfer absorptions

Transfer of electronic charge between ligand and metal orbitals

- transfer of an electron from an orbital with primarily ligand character to one with primarily metal character (ligand-to-metal charge transfer, **LMCT**).
- transfer of an electron from an orbital with primarily metal character to one with primarily ligand character (metal-to-ligand charge transfer, MLCT).

Charge transfer transitions are not restricted by the selection rules that govern ‘d–d ’ transitions.

The probability of these electronic transitions is therefore high, and the absorption bands are therefore intense

Since electron transfer from metal to ligand corresponds to metal oxidation and ligand reduction, an **MLCT** transition occurs when a **ligand** that is easily **reduced** is bound to a **metal** center that is readily **oxidized**.

LMCT occurs when a **ligand** that is easily **oxidized** is bound to a **metal** center (usually one in a high oxidation state) that is readily **reduced**.

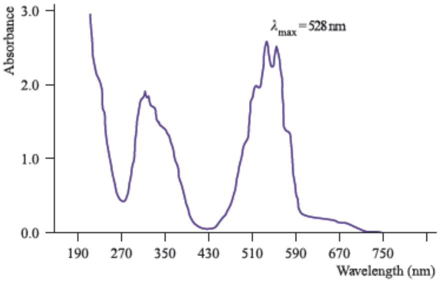

$KMnO_4$. The deep purple color of aqueous solutions of $KMnO_4$ arises from an intense LMCT absorption in the visible part of the spectrum

This transition corresponds to the ***promotion*** of an electron from an orbital that is mainly oxygen lone pair in character to a low-lying, mainly Mn-centered orbital.

$[MnO_4]^-$ (528 nm), $[TcO_4]^-$ (286 nm), $[ReO_4]^-$ (227 nm);

$[CrO_4]^{2-}$ (373 nm), $[MoO_4]^{2-}$ (225 nm), $[WO_4]^{2-}$ (199 nm)

metal center becomes harder to reduce

[FeCl4]2 (220 nm), [FeBr4]2 (244 nm);

ligand becomes easier to oxidize

[OsCl6]3– (282 nm), [OsCl6]2– (370 nm).

Os(IV) being easier to reduce than Os(III).

- Metal-to-ligand charge transfer typically occurs when the ligand has a vacant, low-lying π^* orbital, for example, CO, py, bpy, phen and other heterocyclic, aromatic ligands.
- Often, the associated absorption occurs in the UV region of the spectrum and is not responsible for producing intensely colored species.

the MLCT band may be obscured by the $*\pi\leftarrow\pi$ absorption. For $[Fe(bpy)_3]^{2+}$ and $[Ru(bpy)_3]^{2+}$, the MLCT bands appear in the visible region at 520 and 452 nm, respectively.

metal *d*-orbitals are relatively close in energy to the ligand π^* orbitals

Selection rules

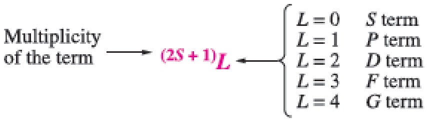

Spin selection rule: $\Delta S = 0$
Transitions may occur from singlet to singlet, or from triplet to triplet states, and so on, but a change in spin multiplicity is ***forbidden***.

Laporte selection rule: There must be a change in parity:
allowed transitions: $g \leftrightarrow u$
forbidden transitions: $g \leftrightarrow g$ $u \leftrightarrow u$
This leads to the selection rule:
$\Delta l = \pm 1$
and, thus, allowed transitions are s ↔ p, p ↔ d, d ↔ f ;
forbidden transitions are s ↔ s, p ↔ p, d ↔ d, f ↔ f ,
s ↔ d, p ↔ f etc.

Absorption maxima in a visible spectrum have three important characteristics

1. number (how many there are)

This depends on the electron configuration of the metal centre

2. position (what wavelength/energy)

This depends on the ligand field splitting parameter, Δ_{oct} or Δ_{tet} and on the degree of inter-electron repulsion

3. intensity

This depends on the "allowedness" of the transitions which is described by two selection rules

A ***spin-forbidden*** transition becomes '**allowed**' if, for example, a singlet state mixes to some extent with a triplet state. This is possible by *spin–orbit coupling.*

for first row metals, the degree of mixing is small and so and is associated with '***spin-forbidden***' transitions are very weak.

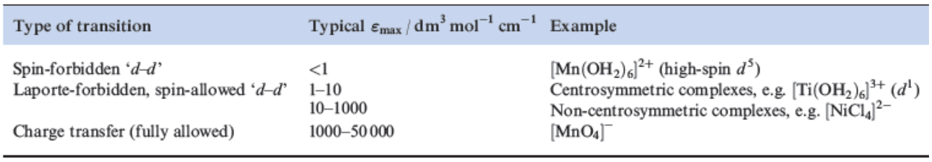

Type of transition	Typical ε_{max} / $dm^3\ mol^{-1}\ cm^{-1}$	Example
Spin-forbidden '*d–d*'	<1	$[Mn(OH_2)_6]^{2+}$ (high-spin d^5)
Laporte-forbidden, spin-allowed '*d–d*'	1–10	Centrosymmetric complexes, e.g. $[Ti(OH_2)_6]^{3+}$ (d^1)
	10–1000	Non-centrosymmetric complexes, e.g. $[NiCl_4]^{2-}$
Charge transfer (fully allowed)	1000–50 000	$[MnO_4]^-$

Spin-allowed 'd–d' transitions remain **Laporte-forbidden** and their observation is explained by a mechanism called "vibronic coupling"

An octahedral complex possesses a center of symmetry, but molecular vibrations result in its temporary loss. At an instant when the molecule does not possess a center of symmetry, mixing of ***d*** and ***p*** orbitals can occur.

In a molecule which is noncentrosymmetric (e.g. tetrahedral), ***p–d*** mixing can occur to a greater extent and so the probability of 'd–d' transitions is greater than in a centrosymmetric complex.

Tetrahedral complexes being more intensely colored than octahedral complexes.

Worked example 21.3 Spin-allowed and spin-forbidden transitions

Explain why an electronic transition for high-spin $[Mn(OH_2)_6]^{2+}$ is spin-forbidden, but for $[Co(OH_2)_6]^{2+}$ is spin-allowed.

$[Mn(OH_2)_6]^{2+}$ is high-spin d^5 Mn(II):

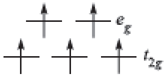

$[Co(OH_2)_6]^{2+}$ is a high-spin d^7 Co(II) complex:

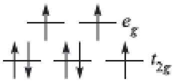

Electronic spectra of octahedral and tetrahedral complexes

For high-spin complexes octahedral d^1 ion $[Ti(OH_2)_6]^{3+}$

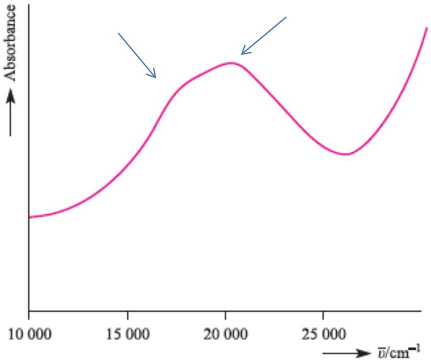

Ti^{3+} (**d^1**, one electron with L = 2, S = 1/2) is ^2D.

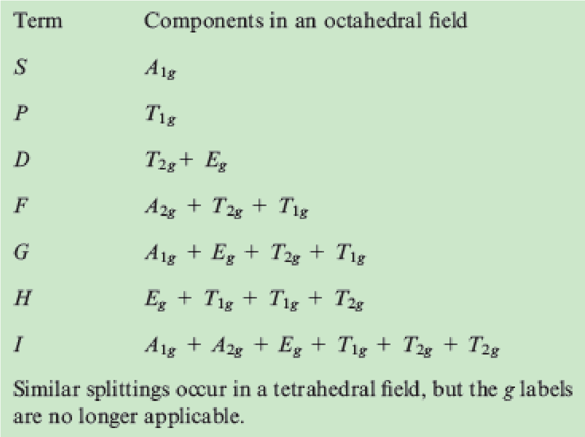

Term	Components in an octahedral field
S	A_{1g}
P	T_{1g}
D	$T_{2g} + E_g$
F	$A_{2g} + T_{2g} + T_{1g}$
G	$A_{1g} + E_g + T_{2g} + T_{1g}$
H	$E_g + T_{1g} + T_{1g} + T_{2g}$
I	$A_{1g} + A_{2g} + E_g + T_{1g} + T_{2g} + T_{2g}$

Similar splittings occur in a tetrahedral field, but the *g* labels are no longer applicable.

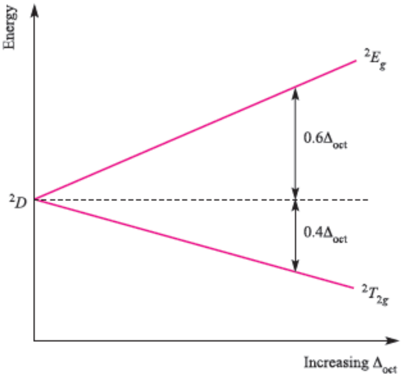

Energy level diagram for a **d^1** ion in an octahedral field.

For the d^1 ion, two possible configurations:
$t_{2g}1\,e_g^0$ or $t_{2g}^0\,e_g^1$, and these give rise to the $^2T_{2g}$ (ground state) and ^2E_g (excited state) terms.

electronic spectrum of $[Ti(OH_2)_6]^{3+}$ consists of two bands, rather than one!!!!!!!

Jahn–Teller effect in the excited state

The d^9 and d^1 configurations are related by a ***positive hole concept***

- ***d***^{9} is derived from a ***d***^{10} configuration by replacing one electron by a positive hole
- For a ***d***^{9} ion in an octahedral field, the splitting diagram is an inversion of that for the octahedral ***d***^{1} ion

In the weak-field limit, a ***d***^{5} ion is high-spin and spherically symmetric, and in this latter regard, ***d***^{0}, ***d***^{5} and ***d***^{10} configurations are analogous.

Addition of one electron to the high-spin ***d*****^{5}** ion to give a ***d*****^{6}** configuration mimics going from a ***d*****^{0}** to ***d*****^{1}** configuration

Likewise, going from ***d*****^{5}** to ***d*****^{4}** by adding a positive hole mimics going from ***d*****^{10}** to ***d*****^{9}**

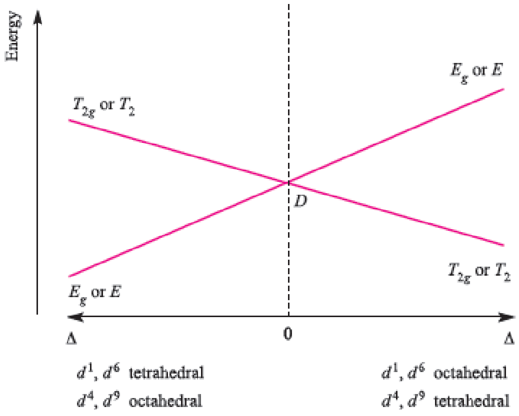

Orgel diagram

- for octahedral d^1 and d^6, the transition is $E_g \leftarrow T_{2g}$
- for octahedral d^4 and d^9, the transition is $T_{2g} \leftarrow E_g$

- for tetrahedral d^1 and d^6, the transition is $T_2 \leftarrow E$
- for tetrahedral d^4 and d^9, the transition is $E \leftarrow T_2$

Each transition is spin-allowed

notation for the transitions given above should include ***spin multiplicities***

- d^4 , the transition is ${}^5T_{2g} \leftarrow {}^5E_g$

d^2 configuration

In an absorption spectrum,

- we are concerned with electronic transitions from the ***ground state*** to one or more ***excited states***.
- Transitions are possible from ***one excited state*** to another, but their probability is so low that they can be ignored

- selection rules restrict electronic transitions to those between terms with the same multiplicity;
- the ground state will be a term with the highest spin multiplicity

terms of maximum spin multiplicity

For the d^2 ion, we therefore focus on the ^3F and ^3P (triplet) terms.

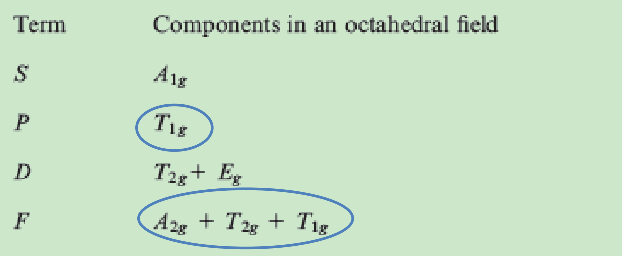

Term	Components in an octahedral field
S	A_{1g}
P	T_{1g}
D	$T_{2g} + E_g$
F	$A_{2g} + T_{2g} + T_{1g}$

The $^3T_{1g}$(F) term corresponds to a $t_{2g}^2e_g^0$ arrangement and is triply degenerate because there are three ways of placing two electrons (with parallel spins) in any two of the d_{xy}, d_{yz} and d_{xz} orbitals

The $^3A_{2g}$ term corresponds to $t_{2g}^0e_g^2$ arrangement (singly degenerate).

The $^3T_{2g}$ and $^3T_{1g}$**(P)** terms equate with a $t_{2g}^1e_g^1$ configuration; the lower energy $^3T_{2g}$ term arises from placing two electrons in orbitals lying in mutually perpendicular planes, e.g. $(d_{xy})^1(d_{z^2})^1$,

while the higher energy $^3T_{1g}$(P) term arises from placing two electrons in orbitals lying in the same plane e.g. $(d_{xy})^1(d_{x^2\ y^2})^1$.

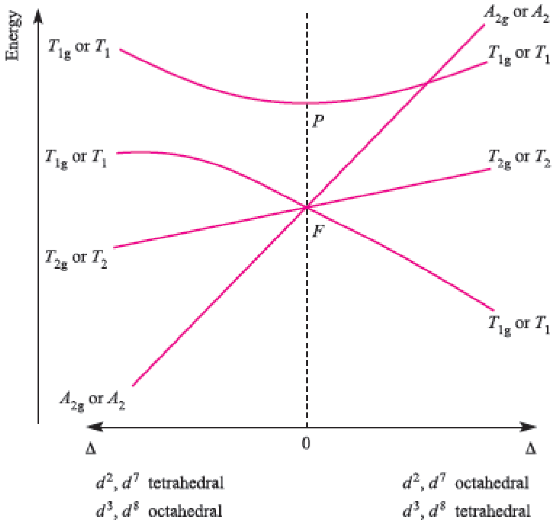

for an octahedral ***d*^{3}** ion, the allowed transitions are

${}^4T_{2g} \leftarrow {}^4A_{2g}$,
${}^4T_{1g}(F) \leftarrow {}^4A_{2g}$
$4T_{1g}$(P) ← ${}^4A_{2g}$.

spin-allowed

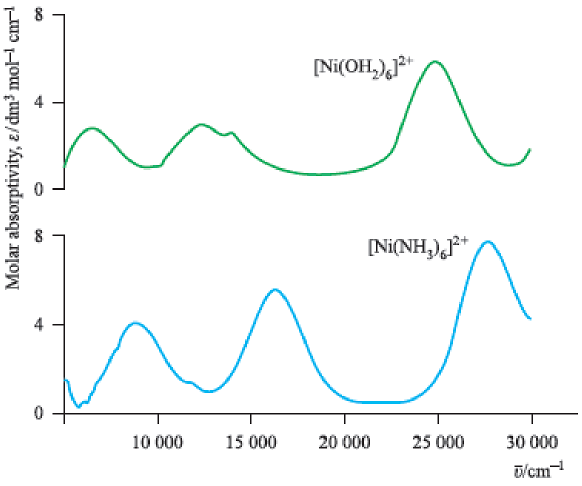

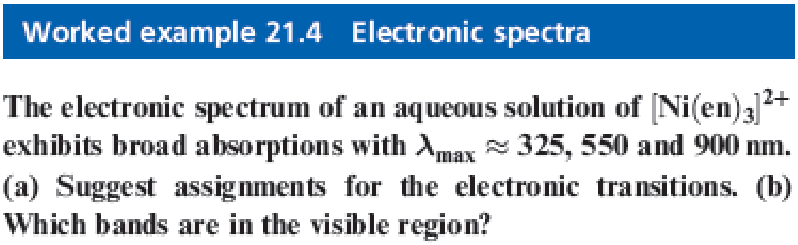

Worked example 21.4 Electronic spectra

The electronic spectrum of an aqueous solution of $[Ni(en)_3]^{2+}$ exhibits broad absorptions with $\lambda_{max} \approx 325$, 550 and 900 nm. (a) Suggest assignments for the electronic transitions. (b) Which bands are in the visible region?

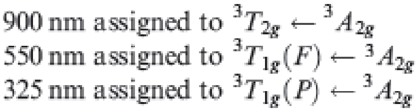

900 nm assigned to ${}^3T_{2g} \leftarrow {}^3A_{2g}$
550 nm assigned to ${}^3T_{1g}(F) \leftarrow {}^3A_{2g}$
325 nm assigned to ${}^3T_{1g}(P) \leftarrow {}^3A_{2g}$

Interpretation of electronic spectra: use of Racah parameters

For a ***d^1*** configuration, the energy of the absorption band in an electronic spectrum gives a direct measure of Δ_{oct}.

How do we determine a value of Δ_{oct} from such a spectrum?

For a given electron configuration, the energies of the terms are given by equations involving ***Racah*** parameters (A, B and C) which allow for ***electron–electron*** repulsions.

These parameters are used in addition to Δ_{oct} to quantify the description of the spectrum from a ***d***^{2} configuration,

$$\text{Energy of } {}^1S = A + 14B + 7C$$
$$\text{Energy of } {}^1D = A - 3B + 2C$$
$$\text{Energy of } {}^1G = A + 4B + 2C$$
$$\text{Energy of } {}^3P = A + 7B$$
$$\text{Energy of } {}^3F = A - 8B$$

The actual energies of the terms can be determined spectroscopically and the ordering is found to be
$^3F < {}^1D < {}^3P < {}^1G < {}^1S$.
Compare this with a predicted ordering from Hund's rules of
$^3F < {}^3P < {}^1G < {}^1D < {}^1S$:

Interpretation of electronic spectra:Tanabe-Sugano diagram

The energy of the ground state is taken to be zero for all field strengths, and the energies of all other terms and their components are plotted with respect to the ground term.

energy and field strength are both expressed in terms of the ***Racah*** parameter B

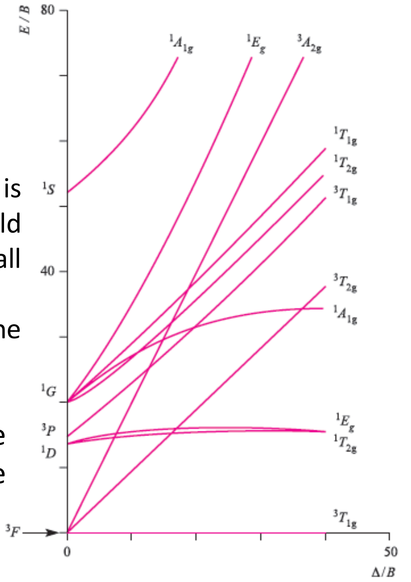

Tanabe–Sugano diagram for the d^2 configuration in an octahedral field.

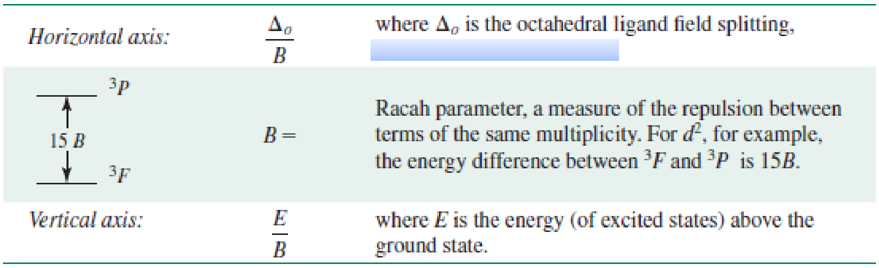

Horizontal axis:	$\frac{\Delta_o}{B}$	where Δ_o is the octahedral ligand field splitting,
^3P 15 B ^3F	$B =$	Racah parameter, a measure of the repulsion between terms of the same multiplicity. For d^2, for example, the energy difference between ^3F and ^3P is $15B$.
Vertical axis:	$\frac{E}{B}$	where E is the energy (of excited states) above the ground state.

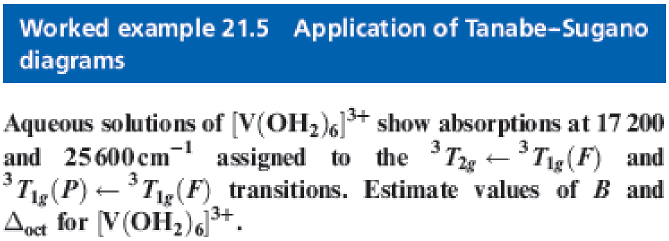

Worked example 21.5 Application of Tanabe–Sugano diagrams

Aqueous solutions of $[V(OH_2)_6]^{3+}$ show absorptions at 17 200 and 25 600 cm^{-1} assigned to the $^3T_{2g} \leftarrow {}^3T_{1g}(F)$ and $^3T_{1g}(P) \leftarrow {}^3T_{1g}(F)$ transitions. Estimate values of B and Δ_{oct} for $[V(OH_2)_6]^{3+}$.

$[V(OH_2)_6]^{3+}$ is a d^2

Only approximate values of **B** and Δ_{oct} can be obtained

Let the transition energies be E_2 = 25 600 cm^{-1} and E_1 = 17 200 cm^{-1}.

ratios of energies can be obtained

$$\frac{\left(\frac{E_2}{B}\right)}{\left(\frac{E_1}{B}\right)} = \frac{E_2}{E_1}$$

From the observed absorption data:

$$\frac{E_2}{E_1} = \frac{25\,600}{17\,200} = 1.49$$

We now proceed by trial and error, looking for the value of $\frac{\Delta_{\text{oct}}}{B}$ which corresponds to a ratio

$$\frac{\left(\frac{E_2}{B}\right)}{\left(\frac{E_1}{B}\right)} = 1.49$$

Trial points:

$$\text{when } \frac{\Delta_{\text{oct}}}{B} = 20, \qquad \frac{\left(\frac{E_2}{B}\right)}{\left(\frac{E_1}{B}\right)} \approx \frac{32}{18} = 1.78$$

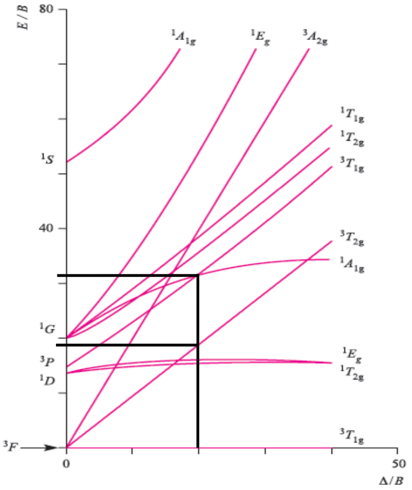

$$\text{when } \frac{\Delta_{\text{oct}}}{B} = 30, \qquad \frac{\left(\frac{E_2}{B}\right)}{\left(\frac{E_1}{B}\right)} \approx \frac{41}{28} = 1.46$$

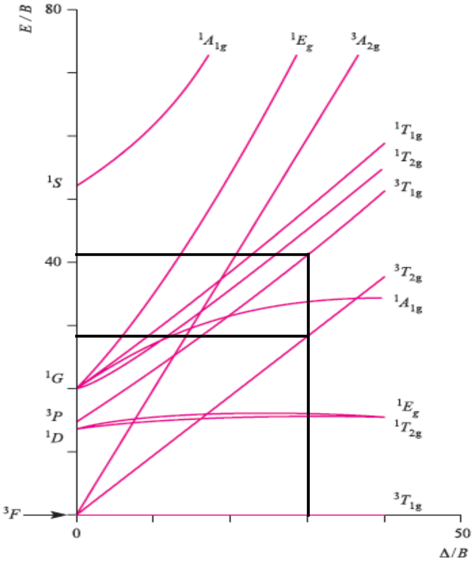

when $\frac{\Delta_{\text{oct}}}{B} = 29$, $\qquad \frac{\left(\frac{E_2}{B}\right)}{\left(\frac{E_1}{B}\right)} \approx \frac{40.0}{26.9} = 1.49$

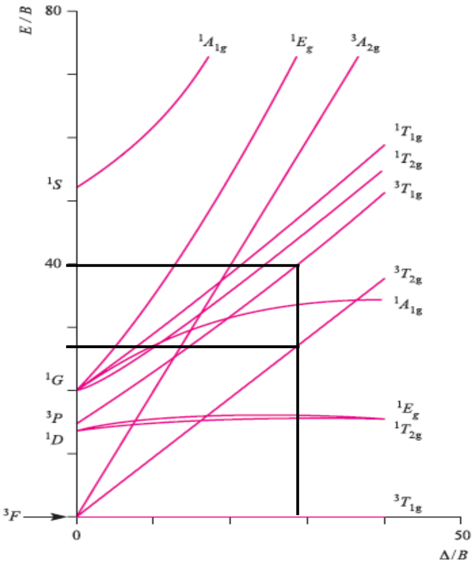

This is an approximate answer but we are now able to estimate B and Δ_{oct} as follows:

- when $\frac{\Delta_{\text{oct}}}{B} = 29$, we have $\frac{E_2}{B} \approx 40.0$, and since $E_2 = 25\,600\,\text{cm}^{-1}$, $B \approx 640\,\text{cm}^{-1}$;
- when $\frac{\Delta_{\text{oct}}}{B} = 29$, $\frac{E_1}{B} \approx 26.9$, and since $E_1 = 17\,200\,\text{cm}^{-1}$, $B \approx 640\,\text{cm}^{-1}$.

Substitution of the value of B into $\frac{\Delta_{\text{oct}}}{B} = 29$ gives an estimate of $\Delta_{\text{oct}} \approx 18\,600\,\text{cm}^{-1}$.

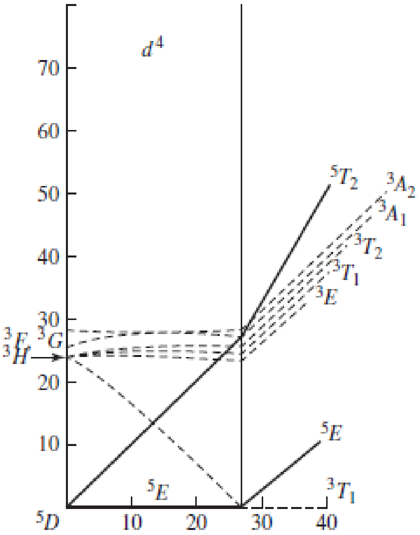

Q1. Determine the ground terms for the following configurations:

a. d^8 (O_h symmetry)

b. high-spin and low-spin d^5 (O_h symmetry)

c. d^4 (T_d symmetry)

d. d^9 (D_{4h} symmetry, square@planar)

$^3F_4$

$^6S_{5/2}$ $^2I_{11/2}$, $^2I_{13/2}$

$^5D_0$

$^2D_{5/2}$

$[Co(NH_3)_6]^{2+}$ has absorption bands at 9,000 and 21,100 cm^{-1} . Calculate Δ_o and *B* for this ion. (Hints: The ${}^4T_{1g} \rightarrow {}^4A_{2g}$ transition in this complex is too weak to be observed.

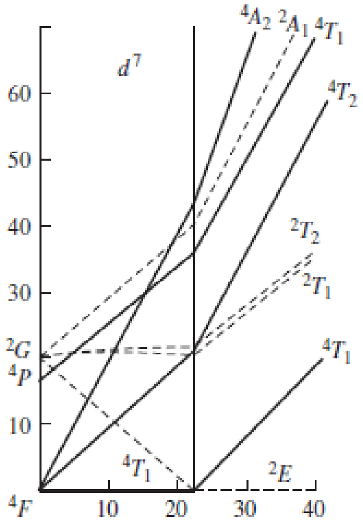

$\nu_2/\nu_1 = 2.34$ at $\Delta_o/B = 11$. From the Tanabe-Sugano diagram at $\Delta_o = 11$,

ν_1: $E/B = 10$ $E = 10\ B = 9{,}000\ cm^{-1}$ $B = 900\ cm^{-1}$

ν_2: $E/B = 22.5$ $E = 22.5\ B = 21{,}100\ cm^{-1}$ $B = 938\ cm^{-1}$

Average $B = 919\ cm^{-1}$, $\Delta_o = 11\ B = 10{,}100\ cm^{-1}$

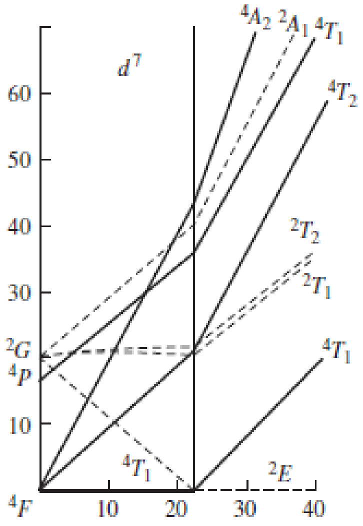

Evidence for metal-ligand covalent bonding

The *nephelauxetic* effect

Nephelauxetic means (electron) 'cloud expanding'.

- Pairing energies are lower in complexes than in gaseous M^{n+} ions, indicating that interelectronic repulsion is less in complexes and that the effective size of the metal orbitals has increased.

$$\mathrm{F^- < H_2O < NH_3 < en < [ox]^{2-} < [NCS]^- < Cl^- < [CN]^- < Br^- < I^-}$$

$$\xrightarrow[\text{increasing nephelauxetic effect}]{\qquad\qquad\qquad\qquad\qquad\qquad}$$

independent of metal ion:

$$\mathrm{Mn(II) < Ni(II) \approx Co(II) < Mo(II) < Re(IV) < Fe(III)}$$
$$\mathrm{< Ir(III) < Co(III) < Mn(IV)}$$

$$\xrightarrow[\text{increasing nephelauxetic effect}]{\qquad\qquad\qquad\qquad\qquad\qquad}$$

Selected values of ***h*** and ***k*** which are used to parameterize the nephelauxetic series

Metal ion	*k*	Ligands	*h*
Co(III)	0.35	6 Br^-	2.3
Rh(III)	0.28	6 Cl^-	2.0
Co(II)	0.24	6 $[CN]^-$	2.0
Fe(III)	0.24	3 en	1.5
Cr(III)	0.21	6 NH_3	1.4
Ni(II)	0.12	6 H_2O	1.0
Mn(II)	0.07	6 F^-	0.8

$$\frac{B_0 - B}{B_0} \approx h_{\text{ligands}} \times k_{\text{metal ion}}$$

B Racah parameter; B_0 is the interelectronic repulsion in the gaseous M^{n+} ion.

Eq. estimate the reduction in electron–electron repulsion upon complex formation

Electron paramagnetic resonance (EPR) spectroscopy

EPR is used to study paramagnetic species with one or more unpaired electrons, e.g.

- free radicals
- diradicals
- metal complexes containing paramagnetic metal centers
- defects in semiconductors
- irradiation effects in solids
- diamagnetic materials are EPR silent,
- paramagnetic species always exhibit an EPR spectrum.

EPR spectrum consists of one or more lines, depending on the interactions between the ***unpaired electron*** (which acts as a 'probe') and the ***molecular framework*** in which it is located.

Analysis of the shape of the EPR spectrum (the number and positions of EPR lines, and their intensities and line widths) provides information about the paramagnetic species, e.g.

- the structure of a free radical,
- characterization of the coordination sphere around the metal center in a coordination complex,
- the presence of multiple paramagnetic species.

Application of EPR to mononuclear, metal-containing systems.

For a paramagnetic metal ion such as Ti^{3+} (d^1), V^{4+} (d^1) or Cu^{2+} (d^9) with a single unpaired electron,

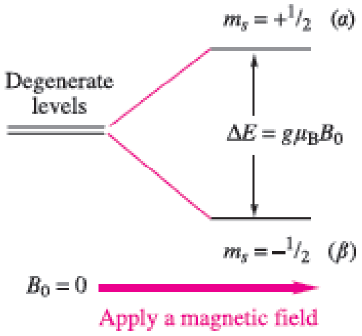

This is called the Zeeman electronic effect and the energy difference, ΔE, is given by:

$$\Delta E = g\mu_B B_0$$

where g is the Lande´ *g*-factor (*g*-value)
μ_B is the Bohr magneton ($1\mu_B = eh/4\pi m_e = 9.274\times 10^{-24}\,\mathrm{J\,T^{-1}}$),
B_0 is the applied magnetic field.

Since g is given by the ratio $2\mu_e/\mu_B$, it is dimensionless, and is equal to 2.0023 for a free electron.

For a metal ion, ***spin–orbit coupling*** leads to ***g*-values** that are significantly different from that of a free electron.

21.9 Magnetic properties

Magnetic susceptibility

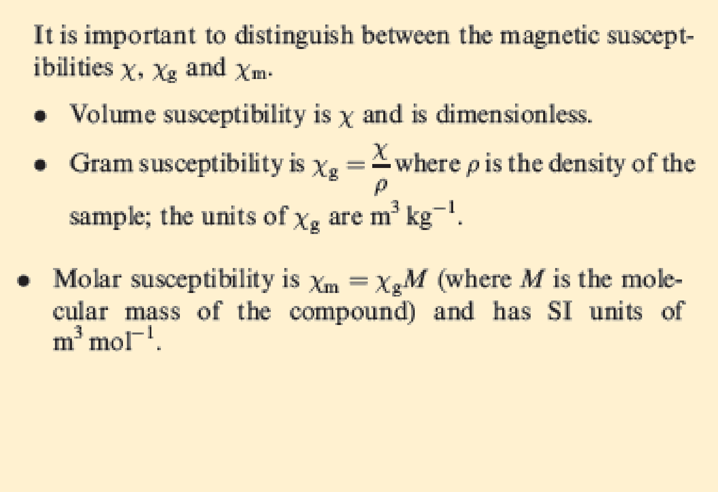

It is important to distinguish between the magnetic susceptibilities χ, χ_g and χ_m.

- Volume susceptibility is χ and is dimensionless.
- Gram susceptibility is $\chi_g = \frac{\chi}{\rho}$ where ρ is the density of the sample; the units of χ_g are $\mathrm{m^3\,kg^{-1}}$.
- Molar susceptibility is $\chi_m = \chi_g M$ (where M is the molecular mass of the compound) and has SI units of $\mathrm{m^3\,mol^{-1}}$.

Magnetic susceptibility and the spin-only formula

- Paramagnetism arises from unpaired electrons.
- Each electron has a ***magnetic moment*** with one component associated with the spin angular momentum of the electron and a second component associated with the orbital angular momentum.

For many complexes of first row ***d***-block metal ions we can ignore the second component and the **magnetic moment**, μ, can be regarded as being determined by the number of *unpaired electrons*, ***n***

$$\mu(\text{spin-only}) = 2\sqrt{S(S+1)} \qquad (21.15)$$

$$\mu(\text{spin-only}) = \sqrt{n(n+2)} \qquad (21.16)$$

The effective magnetic moment, μ_{eff} , can be obtained from the experimentally measured ***molar magnetic susceptibility***, χ_m

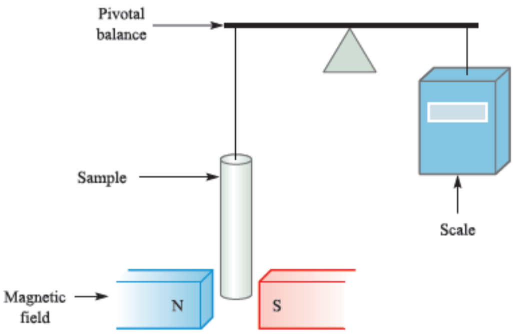

Schematic representation of a Gouy balance.

Gouy method makes use of the interaction between unpaired electrons and a magnetic field.

- A diamagnetic material is repelled by a magnetic field.
- whereas a paramagnetic material is attracted into it.

Spin-only values of $\boldsymbol{\mu_{eff}}$ compared with approximate ranges of observed magnetic moments for *high-spin* complexes of first row ***d***-block ions.

Metal ion	d^n configuration	S	μ_{eff}(spin-only) / μ_B	Observed values of μ_{eff} / μ_B
Sc^{3+}, Ti^{4+}	d^0	0	0	0
Ti^{3+}	d^1	$\frac{1}{2}$	1.73	1.7–1.8
V^{3+}	d^2	1	2.83	2.8–3.1
V^{2+}, Cr^{3+}	d^3	$\frac{3}{2}$	3.87	3.7–3.9
Cr^{2+}, Mn^{3+}	d^4	2	4.90	4.8–4.9
Mn^{2+}, Fe^{3+}	d^5	$\frac{5}{2}$	5.92	5.7–6.0
Fe^{2+}, Co^{3+}	d^6	2	4.90	5.0–5.6
Co^{2+}	d^7	$\frac{3}{2}$	3.87	4.3–5.2
Ni^{2+}	d^8	1	2.83	2.9–3.9
Cu^{2+}	d^9	$\frac{1}{2}$	1.73	1.9–2.1
Zn^{2+}	d^{10}	0	0	0

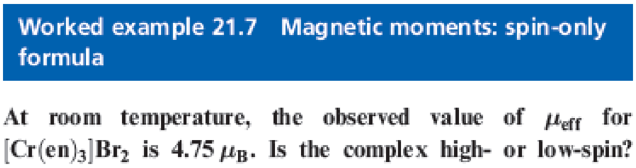

Worked example 21.7 Magnetic moments: spin-only formula

At room temperature, the observed value of μ_{eff} for $[Cr(en)_3]Br_2$ is 4.75 μ_B. Is the complex high- or low-spin?

Cr^{2+} (d^4) ion.
Low-spin will have two unpaired electrons (n = 2).
High-spin will have four (n = 4).
Assume that thse pin-only formula is valid (first row metal, octahedral complex):

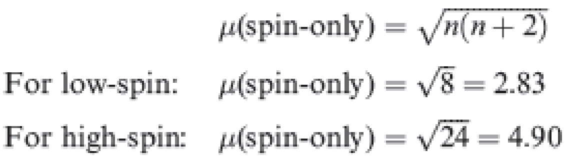

$$\mu(\text{spin-only}) = \sqrt{n(n+2)}$$

For low-spin: $\mu(\text{spin-only}) = \sqrt{8} = 2.83$

For high-spin: $\mu(\text{spin-only}) = \sqrt{24} = 4.90$

Spin and orbital contributions to the magnetic moment

moments arising from both the spin and orbital angular momenta contribute to the observed magnetic moment.

The energy difference between adjacent states with ***J*** values of ***J'*** and ***(J' + 1)*** is given by the expression **(*J'* + 1)**λ where λ is called the ***spin–orbit coupling constant***.

For the ***d*²** configuration, for example, the ^3F term in an octahedral field is split into $^3F_2$, $^3F_3$ and $^3F_4$, the energy differences between successive pairs being 3 and 4 respectively

In a magnetic field, each state with a different ***J*** value splits again to give **(*2J* + 1)** different levels separated by $g_J\mu_B B_0$ where g_J is a constant called the Lande´ splitting factor and B_0 is the magnetic field.
It is the very small energy differences between these levels with which **EPR** spectroscopy is concerned and *g*-values are measured using this technique

The value of λ varies from a fraction of a cm^{-1} for the very lightest atoms to a few thousand cm^{-1} for the heaviest ones.

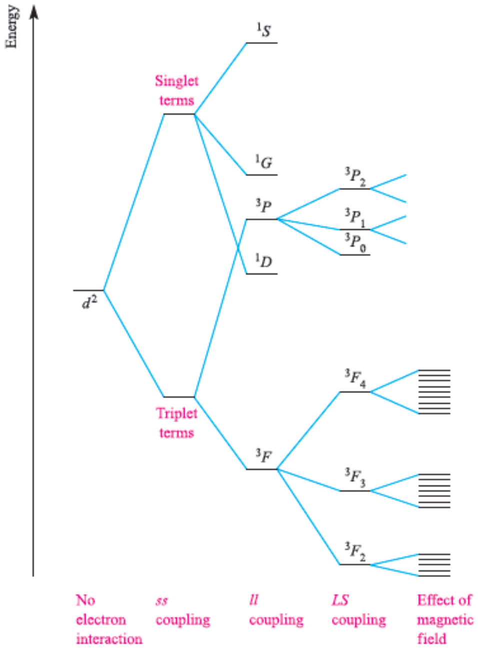

For many (but not all) first row metal ions, λ is very small and the spin and orbital angular momenta of the electrons operate independently.

spin–orbit coupling

As a result of spin–orbit coupling, mixing of terms occurs. Thus, for example, the $^3A_{2g}$ ground term of an octahedral d^8 ion (Figure 21.20) mixes with the higher $^3T_{2g}$ term.

The extent of mixing is related to Δ_{oct} and to the spin–orbit coupling constant, λ .

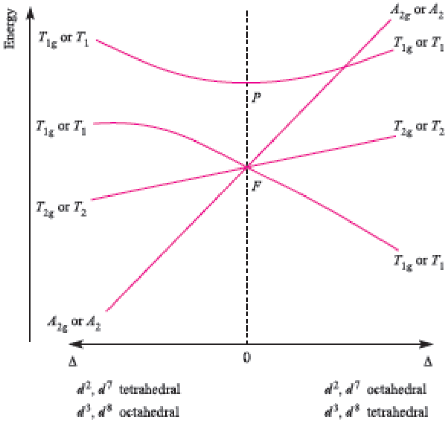

Table 21.13 Spin–orbit coupling coefficients, λ, for selected first row *d*-block metal ions.

Metal ion	Ti^{3+}	V^{3+}	Cr^{3+}	Mn^{3+}	Fe^{2+}	Co^{2+}	Ni^{2+}	Cu^{2+}
d^n configuration	d^1	d^2	d^3	d^4	d^6	d^7	d^8	d^9
λ/cm^{-1}	155	105	90	88	−102	−177	−315	−830

$$\mu_{\text{eff}} = \mu(\text{spin-only})\left(1 - \frac{\alpha\lambda}{\Delta_{\text{oct}}}\right)$$

$$= \sqrt{n(n+2)}\left(1 - \frac{\alpha\lambda}{\Delta_{\text{oct}}}\right)$$

where: λ = spin–orbit coupling constant

$\alpha = 4$ for an A ground term

$\alpha = 2$ for an E ground term

- $\mu_{\text{eff}} > \mu(\text{spin-only})$ for d^6, d^7, d^8 and d^9 ions;
- $\mu_{\text{eff}} < \mu(\text{spin-only})$ for d^1, d^2, d^3 and d^4 ions.

Worked example 21.8 Magnetic moments: spin–orbit coupling

Calculate a value for μ_{eff} for $[\text{Ni(en)}_3]^{2+}$ taking into account spin–orbit coupling. Compare your answer with μ(spin-only) and the value of $3.16\,\mu_B$ observed experimentally for $[\text{Ni(en)}_3][\text{SO}_4]$. [Data: see Tables 21.2 and 21.13.]

Octahedral Ni(II) (d^8) has a ${}^3A_{2g}$ ground state. Equation needed:

$$\mu_{\text{eff}} = \mu(\text{spin-only})\left(1 - \frac{4\lambda}{\Delta_{\text{oct}}}\right)$$

$$\mu(\text{spin-only}) = \sqrt{n(n+2)} = \sqrt{8} = 2.83$$

From Table 21.2: $\Delta_{\text{oct}} = 11\,500\ \text{cm}^{-1}$
From Table 21.13: $\lambda = -315\ \text{cm}^{-1}$

$$\mu_{\text{eff}} = 2.83\left(1 + \frac{4 \times 315}{11\,500}\right) = 3.14\,\mu_B$$

The effects of temperature on μ_{eff}

When spin–orbit coupling is large, μ_{eff} is highly dependent on T. Remember that μ is small for first row metal ions, is large for a second row metal ion, and is even larger for a third row ion.

$$\chi = \frac{C}{T}$$

where: C = Curie constant
T = temperature in K

Spin crossover

This may be initiated by a change in pressure (e.g. a low- to high-spin crossover for $[Fe(CN)_5(NH_3)]^{3-}$ at high pressure) or temperature (e.g. octahedral $[Fe(phen)_2(NCS\text{-}N)_2]$,

The change in the value of μ_{eff} which accompanies the spin crossover may be gradual or abrupt

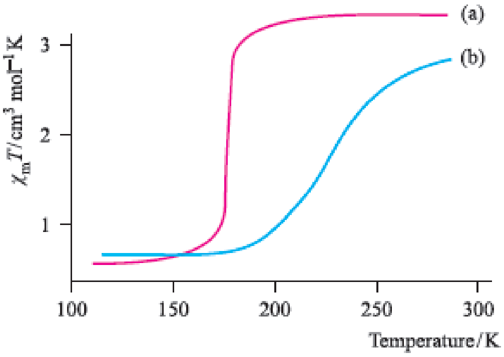

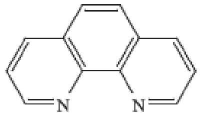

phen = 1,10-phenanthroline

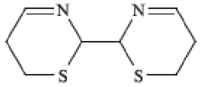

btz = 2,2′-bi-4,5-dihydrothiazine

The dependence of the observed values of μ_{eff} on temperature for
(a) $[Fe(phen)_2(NCS\text{-}N)_2]$ where low- to high-spin crossover occurs abruptly at 175 K, and
(b) $[Fe(btz)_2(NCS\text{-}N)_2]$ where low- to high-spin crossover occurs more gradually.

Ferromagnetism, antiferromagnetism and ferrimagnetism

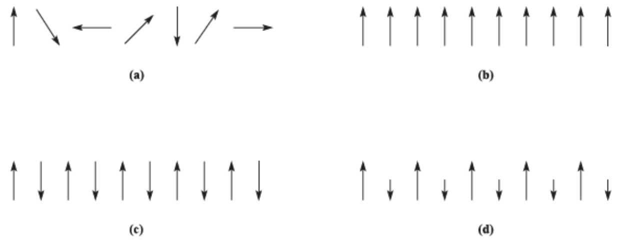

Fig. 21.30 Representations of (a) paramagnetism, (b) ferromagnetism, (c) antiferromagnetism and (d) ferrimagnetism.

In a ***ferromagnetic*** material, large domains of magnetic dipoles are aligned in the same direction;
in an ***antiferromagnetic*** material, neighbouring magnetic dipoles are aligned in opposite directions.

Ferromagnetism leads to greatly enhanced *paramagnetism* as in iron metal at temperatures of up to 1043K